The growth and electrical properties of tin oxide crystals

R. N. S. M. Mehdi

THE GROWTH AND ELECTRICAL PROPERTIES OF TIN OXIDE CRYSTALS

by

R.N.S.M. MEHDI, B.Sc.(Hons), M.Sc.(KARACHI)

Thesis Submitted for the Degree of Master of Science

Faculty of Science

University of Durham

May 1969

A C K N O W L E D G E M E N T S

The author would like to express his thanks to:-

Professor D.A. Wright for his continued guidance and encouragement, for providing initial ideas, and for the use of the facilities of the Department of Applied Physics.

The department workshop staff under the leadership of Mr. Frank Spence for their valuable help and for their skill in building the apparatus.

All members of the Applied Physics Department for their assistance and helpful discussions and especially Dr. D.F. Crabtree for his keen interest in this research programme.

The Commonwealth Scholarship Commission in the United Kingdom, for the award of a scholarship under which this work was performed.

C O N T E N T S

Figure 0.1

A. Crystals grown by Method A

B. Plates grown by Method C at 1275°C

C. Antimony doped crystals, and needles by Method B

D. Colourless undoped Crystalline Mass produced by Method C

Scale: 0 10 20 MM

Figure 0.2

A. Antimony doped crystals and plate grown by Method C

B. Some undoped reduced crystals

See CHAPTER 2

Scale : 0 12 24 MM

CHAPTER 1

INTRODUCTION

The primary purpose of studying stannic oxide was to assess its possibilities as a high mobility material at low temperature.

Although there had been many papers published on thin films, polycrystalline samples and single crystals, no definite information has been known about the scattering mechanism.

In order to obtain as much information as possible on stannic oxide, it was decided to grow single crystals by different methods. This was followed by the measurement of their electrical parameters, optical absorption and the observation of luminescence and electroluminescence.

Chapter 2 is a summary of the crystal growth. The first half of the chapter contains the different methods adopted by different workers for the growth. In the second part is given, in brief, the present method and its extension for the preparation of the crystals.

Chapter 3 contains the review of the stannic

oxide work in detail. In the beginning some relevant theory of electron scattering mechanism is also described.

The apparatus and the experimental techniques employed are described in detail in Chapter 4. It also deals with the electrical measurement data. Reference is made to experimental results wherever necessary to preserve continuity and avoid repetition later.

The optical absorption results are presented in Chapter 5 together with luminescence and electroluminescence. The experimental set up for the above mentioned effects is also described.

The discussion on the experimental results is given in Chapter 6. Some theoretical interpretation of the results is also mentioned. The conclusions and suggestions are given at the end of the chapter.

CHAPTER 2

CRYSTAL GROWTH

Section 1 Introduction

Stannic oxide cannot be grown directly from the melt because it sublimes at temperature above about 1500°C, and the melting point is in the region of 2500°C.

Section 2 Growth from the Liquid Phase

(a) Fluxed Melt

One of the simplest methods of growing crystals is that from a saturated solution. Since there is no known room temperature solvent for stannic oxide, a brief survey was made by MORGAN (5) of different fluxes that have been used for growing similar materials at high temperatures. PbO, PbF_2, $PbCl_2$, KF, KCl, B_2O_3, $CaCl_2$ were used as fluxes. The general procedure was to put the salt with 20% by weight of SnO_2 powder in a platinum crucible and heat to about 1200°C for 2 to 4 hours. The only partial success was obtained with a flux of lead oxide. A few very small reddish crystals were obtained.

KUNKLE and KOHNKE (6) grew good crystals of stannic oxide with sizes up to 1 x 1 x 5 to 10 mm from Cu_2O

flux. These crystals were colourless, having resistivities in the range of 10^9 - 10^{10} ohm cm.

The main advantages of the process are

(i) growth at temperatures below the solute melting points

(ii) high quality crystals are obtainable

(iii) doping with suitable elements is readily achieved.

There are some disadvantages in this method, such as contamination of the crystal by the solvent constituent elements or, more rarely, by the crucible material.

(b) Hydrothermal Synthesis

Certain materials which are not very soluble in water under normal conditions can become so under conditions of very high pressure and temperature. Under controlled conditions it is possible to obtain crystal growth from this state. KUS'MINA and LITVIN (7) have recently reported the hydrothermal synthesis of stannic oxide from a solvent of LiOH solution at 400 - 600°C and 2000 atmospheres pressure. No information is available on the dimensions or properties of these crystals.

Section 3 Growth from the Vapour Phase

(a) Sublimation in a Closed System

The solid materials, crystalline or

amorphous, may be transported by sublimation through the vapour phase under the influence of temperature gradient. Such direct vapour transport had been used for the growing of crystals.

CLARK and WOODS (8) have grown crystals of cadmium sulphide of high quality and purity by this method. This method was attempted by MORGAN (5) but large crystals could not be obtained. VAN DALL (9) prepared single crystals of stannic oxide from sintered pellets. These were placed in a semi-closed alumina vessel and heated at 1650°C in air. Large crystals were grown on top of the pellets. The impurity content of the crystals especially Aluminium was high. The other impurities as detected by spectrographic analysis were Boron, Iron and Magnesium.

For purer crystals the preparation temperature was reduced. HBr gas was used as a transporting medium, and transport of stannic oxide took place from a low temperature region (800°C) to a high temperature region (900°C).

MANDEL(10) and SCHAFER (11) suggested that the basis of this transport was the rapid establishment of an equilibrium between the solid substrate and the reactive gas.

(b) Hydrolysis of Stannic Chloride

KOCH (12), ISHIGURA (13) and other workers had prepared stannic oxide thin films through a rapid hydrolysis

reaction of stannic chloride, as shown by the following equation, at high temperature

$$SnCl_4 + 2\ H_2O \longrightarrow SnO_2 + 4\ HCl$$

This is accomplished by spraying an alcoholic or hydrochloric aqueous solution of stannic chloride on the surface of substrate heated above 500°C.

NAGASAWA (14) grew single crystals with sizes up to 2 x 5 x 15 mm by the reaction of water and stannic chloride vapours at 1300°C in an electrically heated furnace. These crystals were grown in quartz and also in mullite tubes. A slight amount of Aluminium, which was not present in the crystals grown by using a quartz tube, were detected spectroscopically when mullite tube was used.

MORGAN(5) attempted to grow crystals by a similar method. A large mass of crystalline material was formed, but individual crystals were difficult to separate and orientate. The crystals were white and opaque.

(c) Flame Fusion Method

Stannic oxide can be formed by the hydrolysis of stannic chloride in an oxy-hydrogen flame. This reaction

is similar to equation given in (3b) where the H_2O is formed by the burning of hydrogen in oxygen. Attempts were made by MORGAN (5) but large single crystals could not be grown by this method. However it was possible to grow bunches of dendritic needles.

(d) Helium Flow Method

MARLEY and MACAVOY (15) had obtained the single crystals of stannic oxide with the method of the high temperature decomposition-reoxidation reactions, using high purity stannic oxide powder as starting material.

A platinum - 20% Rhodium wound tube furnace was used. The temperature of the hot zone was maintained at 1650°C. A variety of carrier gases were evaluated, including neutral gases, oxygen, and oxygen in combination with either argon, nitrogen or helium.

Nitrogen or argon in combination with oxygen produced crystals up to 2 x 2 x 25 mm in 24 hours but they were imperfect. Attempts with helium as carrier gas were successful; they were able to grow large (2 x 2 x 30) crystals of good quality.

Studies of etch pits in these crystals by KOFFYBERG (16) showed that they had a dislocation density of 10^4 or 10^5 cm^{-2}. One of the conclusions of MARLEY and MACAVOY

was that crystal habit was very dependent on temperature. With the vaporizing site at 1650 °C, rod formation was confined to an area between 1620 and 1570 °C, twinned plates from 1570 °C to 1460 °C, and needles from 1460 °C to 1300 °C.

Section 4 Argon Flow Method

(a) Growth of Stannic Oxide from Sn Vapour and O_2

REED (17) had obtained crystals of high purity by the method of the vapour reactions of tin vapour with oxygen at 1350 °C.

MORGAN(5) adopted the same method to grow the crystals but at slightly higher temperature. By using tin metal as the starting material, the maximum temperature required for crystal growth was 1450 °C. He obtained the best results using argon as carrier gas. Using helium in place of argon produced only thin needles.

The attempts to dope the crystals with antimony and chromium were successful while no good crystals were obtained using cerium, gallium and indium as dopant.

When the pressure of antimony was high, the crystals grew very quickly, within three days. The carrier densities of these crystals were in the order of 10^{20} cm^{-3}. These crystals

were of dark navy blue colour. At lower concentrations of antimony, both rods and plates were formed but growth was much slower. It took nearly 10 - 14 days. By varying the position of boat carrying antimony into the heating zone, crystals of different carrier densities were grown.

Chromium doped crystals which were red in colour showed a p-type sign of seebeck voltage and were of high resistivity.

Indium doped crystals were yellow in colour with p-type seebeck coefficients but had high resistivity similar to or greater than that of undoped crystals.

The undoped crystals were analysed by mass spectroscopy and were found to contain 5 p.p.m. calcium, 20 p.p.m. aluminium and traces of Si ($\backsim$ 20 p.p.m.) Fe ($\backsim$ 50 p.p.m.) and Na ($\backsim$ 5 p.p.m.).

In the present work three methods were adopted for the crystal growth.

(b) Crystal Growth (A)

A furnace utilizing silicon carbide as electrical heating element was constructed. The furnace arrangements and temperature profile of the furnace are shown in Fig.(1.1). The dimensions of the furnace are given in table (1.1).

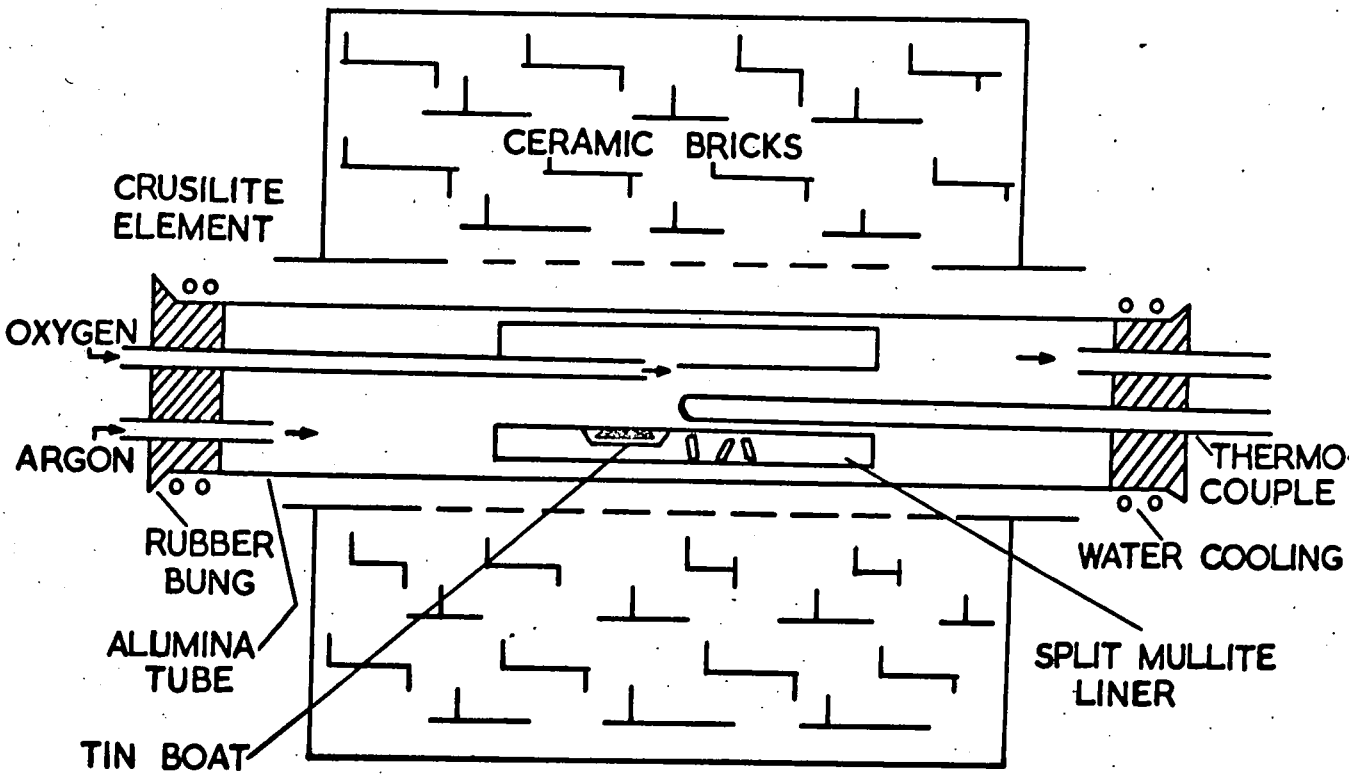

FIG 1·1a

The arrangement of the furnace

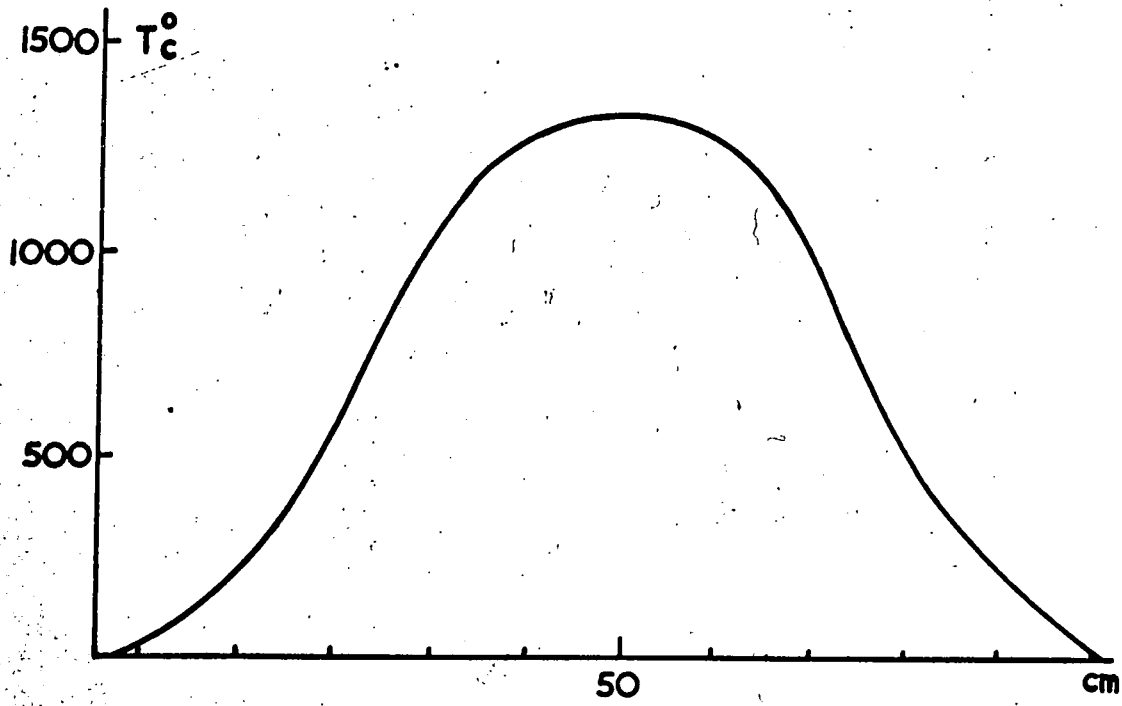

FIG 1·1b

Its temperature profile, used for growing stannic oxide crystals

Height 32 cm	Width 32 cm	Length 56 cm		
Dimensions of tubes and liner	Crucilite element	Alumina tube	Mullite tube	Alumina liner
Length (mm)	650	825	300	300
Internal diameter(mm)	54	38	25	25.5
External diameter(mm)	62	46	32	32
Hot zone(mm)	300		Cut half along diameter	Cut half along diameter
Resistance (ohms)	2.1			

Table 1.1. Dimensions of the Crystal Growing Furnace

The alumina boat containing tin was placed about 10 cm apart from the centre of the furnace, 25 cc/minute of oxygen and 100cc/minute of argon were passed into the tube. The argon was 99.999 % pure. Oxygen and tin, in the vapour phase, diffused into the growing zone situated in the centre of the furnace. The temperature was maintained thermostatically at about 1400 ^{o}C. Platinum - Rhodium 13 % was used as thermocouple.

Two different types of crystals were produced after about thirty six hours depending upon growth region as follows:

(i) growth taking place on the alumina boat or oxygen tube

(ii) growth taking place on the mullite liner.

Crystals growing in region (i) were colourless and transparent, while those grown in region (ii) were either pink or yellow. However discussion on spectrographic analysis of these crystals is given in section (5).

Crystal Growth (B)

As the crystals containing the greatest amount of undesired impurities grew on the mullite liner, this was replaced by an alumina liner and attempts were made, largely without success, to grow crystals under the same conditions as before. Growth of small crystals was however obtained when the

liner and end of oxygen tube were coated with a thin layer of tin oxide before being placed in the system.

Each component was heated in a bunsen flame and while hot ($\sim 450^{\circ}C$) was placed in a jet of vapourised tin chloride. It was observed that crystal growth occurred in the region where tin oxide was deposited. Large transparent undoped crystals with sizes up to 1.5 x 2 x 8 mm were grown. Antimony doping was also carried out.

Crystal Growth (C)

The most satisfactory growth method which was developed was a modification of that due to NAGASAWA (14). The essential features of the furnace were the same as in the previous case except slight alterations which are shown in Fig. (1.2).

Anhydrous stannic chloride and oxygen were used as the suitable compounds for the starting materials of vapour reaction method of stannic oxide crystal growth. The important step in obtaining good crystals was keeping the vapour pressure of the stannic chloride constant. This was done by placing the stannic chloride in a glass vessel dipped in a wash basin filled with hot water at $30^{\circ}C$.

Argon with a rate 50 cc/minute was passed

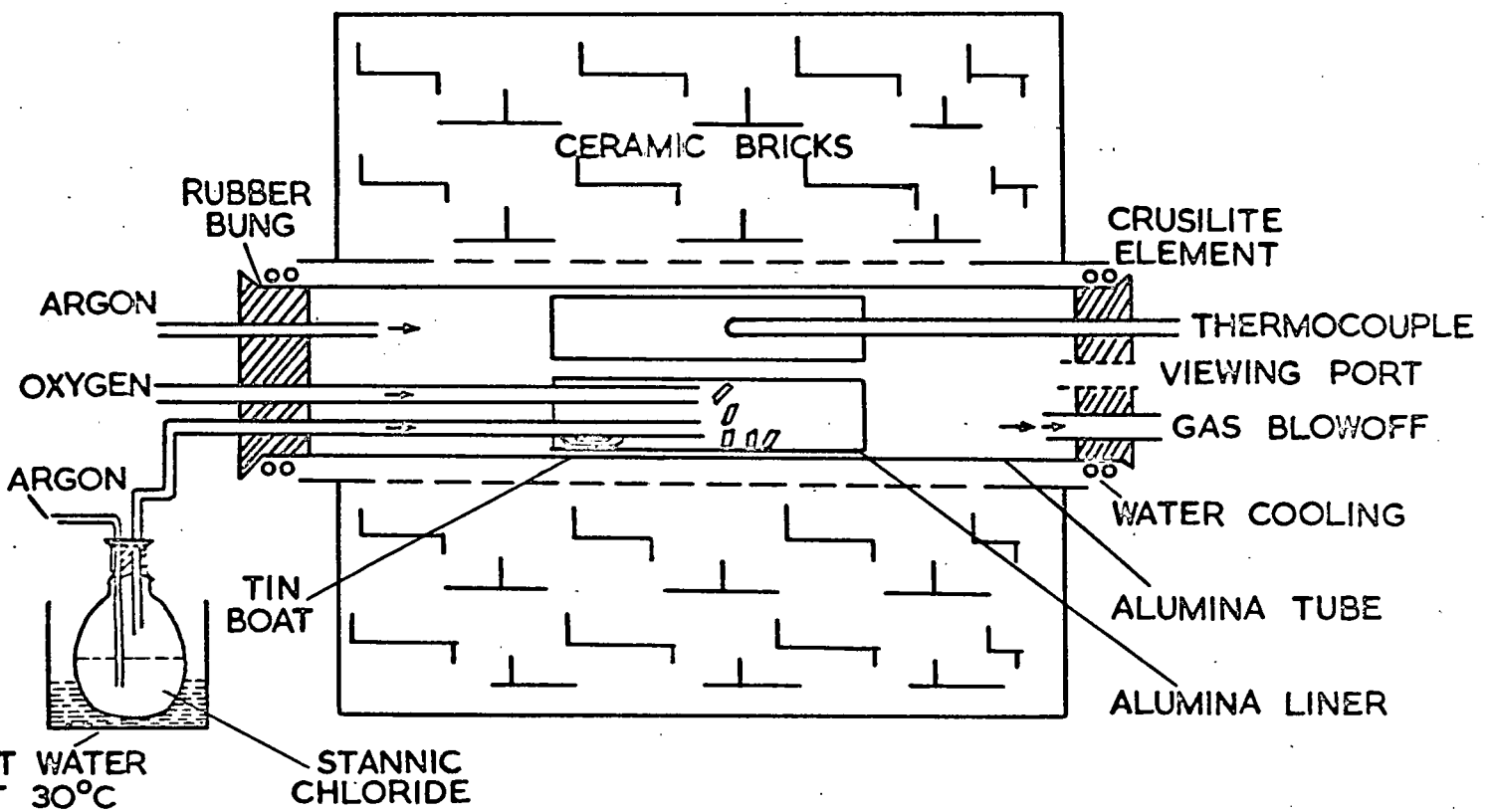

FIG 1·2

The modified arrangement of the furnace for growing stannic oxide crystals

through the glass vessel and subsequently to the lower tube of the furnace to transport stannic chloride vapour into the growing zone. A different rate of argon, 70 cc/minute, was also utilized as a carrier gas through the upper tube of the furnace. Oxygen at a rate of 20 cc/minute was passed to prevent the crystals from becoming too non-stoichiometric.

The following conditions were maintained for growing good crystals:

(i) The temperature of the growing zone was 1400 °C.

(ii) The temperature of the stannic chloride vapour source was about 30 °C.

(iii) Flow rates of different gases were 20, 50, 70 cc/minute.

Single crystals of dimensions up to 2 x 2 x 12 mm grew either in an aggregated mass on the tip of the oxygen tube or on the alumina liner nearest to the tip. The crystals were colourless and transparent and generally having smoothly developed faces. On one occasion some crystals were reddish in colour.

Antimony doped crystals were also obtained by placing Sb_3O_4 in an alumina boat upstream from the boat containing tin pellets and growth took place on the alumina liner. Some of the growth run took only 18 to 19 hours the maximum being

36 hours.

Section 5 Mass Spectrographic Analysis

The crystals grown by Method (A) were sent to Chemical Inspectorate, Royal Arsenal Woolwich who kindly performed a mass spectrographic analysis of them.

The qualitative analysis confirms that crystals grown in region (i) (see crystal growth (A) were of high purity. The only impurities found in both types of specimen were traces of silicon and a very slight trace of sodium.

Those crystals which were grown in region (ii) were either pink or yellow. The pink colour was due to a heavy trace of silicon and traces of calcium, aluminum, magnesium chromium, and iron. The quantitative analysis was as follows:

Pink Crystals

Tin	Major
Silicon	0.3 %
Calcium	0.03%
Aluminum	0.01%
Magnesium	0.02%
Chromium	0.01%
Iron	0.01%

The impurities in yellow crystals were as under:

Yellow Crystals

Tin	Major
Silicon	0.04 - 0.05 %
Indium	0.04 - 0.05 %
Calcium	< 0.002 %
Sodium	< 0.005 %
Copper	< 0.01 %
Aluminum	< 0.01 %
Magnesium	< 0.01 %

When the pink crystals were heated in an oxy-hydrogen flame the colour changed from pink to white and this was probably due to changes in impurity content.

Pink Crystals after Heating

Tin	Major
Silicon	0.1 %
Calcium	0.01%
Aluminum	0.03%
Magnesium	0.01%
Chromium	0.01%
Iron	0.03%

The major changes occurred in the silicon, calcium and iron concentrations.

The tin pellets (starting material) were found to contain only slight traces of lead and bismuth.

No attempts were made to find out the impurity concentrations in crystals grown by the methods (B) and (C).

CHAPTER 3

REVIEW OF THE PREVIOUS WORKS ON STANNIC OXIDE

Section 1 Electron Scattering Mechanism

(a) Introduction

In semiconductors, the most important scattering processes involve interaction of electrons with lattice vibrations and with the impurity atoms. In relatively pure crystals or at relatively high temperatures, the former interaction is ordinarily predominant, while at low temperature, the latter may be more important.

(b) Acoustic Mode Lattice Scattering

Acoustic scattering is important in semiconductors with predominantly covalent type bonding. There are two types of scattering. Deformation potential is the most important as it can occur in any solid. The other type is the piezo-acoustic scattering, which only occurs in crystals that are piezoelectric. Since the structure of stannic oxide has a centre of symmetry, it is not piezoelectric and so piezo-acoustic scattering does not occur.

BARDEEN and SCHOCKLEY (18) solved the

problem of acoustic mode scattering by a deformation potential method. Since the variation in lattice constant produces a change in energy of the band edge, so the longitudinal phonons produce a local dilation that can be interpreted as a change in the band edge, which causes the scattering of the electrons.

The mobility varies as $T^{-3/2}$ and $m^{*-5/2}$. For the fully degenerate situation, the mobility will vary as T^{-1}.

(c) Optical Mode Lattice Scattering

When there are two or more atoms per unit cell, optical modes, in which the two atoms move in opposite directions, are present. If the two atoms are similar, as in elemental semiconductors like Ge, there can be no polarization, but scattering is still caused by the lattice distortion produced. This non polar optical mode scattering has been discussed by HARRISON(3). He expects that at room temperature non polar optical mode scattering would be, in most cases of the same order as acoustic mode scattering.

When two atoms are dissimilar and carry opposite charges as in a polar crystal, their displacement in opposite directions causes an electric polarization of the lattice,

which scatters the electrons. This type of scattering is likely to be predominant in stannic oxide since it is a polar crystal.

A free electron introduced into a polar lattice will cause a distortion of the lattice. The term "polaron" is used to describe the combination of the electron and the distortion. The strength of the interaction between the electrons and the polar modes can be represented by a coupling constant (α_c). Various formulae have been proposed for the mobility, but they are beyond the scope of the present work.

(d) Ionized Impurity Scattering

Ionized impurities in the structure also scatter the charge carriers because the coulomb field associated with each ionized donor or acceptor atom produces an irregularity in the periodic potential. The field of the impurity atom is modified by the dielectric constant of the solid, and the resulting mobility depends upon temperature as the electron velocity is a function of temperature.

The expression for relaxation time τ and hence mobility was derived by BROOKS and HERRING (19).

$$\mu = \frac{e\tau}{m^*} = \frac{64\pi^{\frac{1}{2}} E^2 (2kT)^{3/2}}{N_1 Z^2 e^3 m^{*\frac{1}{2}}} \left\{ \ln \left\{ \frac{24\, m^* k^2 T^2 E}{e^2 h^2 N_I} \right\} \right\}^{-1}$$

where symbols have the usual significance.

In the non-degenerate case if the relatively small variation of the logarithmic term is ignored, the mobility should vary directly as $T^{3/2}$, and inversely as the concentration of impurities.

MANSFIELD (20) obtained an expression for arbitrary degeneracy. For complete degeneracy he showed that the mobility is only dependent on the number of impurities through a logarithmic term and it is independent of temperature.

(e) Neutral Impurity Scattering

At low temperature when most of the impurity atoms are not yet ionized, scattering due to these neutral atoms may occur. This effect has been discussed by PEARSON and BARDEEN (21) and later ERGINSOY (22). The mobility is independent of temperature and is given by

$$\mu_N = \frac{e^3 m^*}{20h^3 N_n}$$

where N_n = concentration of neutral impurity atoms.

(f) Scattering by Dislocations

At low temperature the scattering of electrons

on dislocations (lattice defects) may be important. This could be observed in very pure semiconductors. DEXTER and SEITZ (23) calculated the scattering by dislocations and found that relaxation time and mobility are both proportional to temperature.

$$\mu = DT$$

where $D \propto \frac{1}{N_{dis}}$ N_{dis} being the number of edge dislocating per cm^2.

(g) Electron Electron Scattering

Electron electron scattering does not effect the mobility directly as the total energy before and after a collision is unchanged. However these collisions can redistribute the energy so that other mechanisms can remove it more effectively.

Section 2 Previous Work on Stannic Oxide

(a) Thin Films

The earliest electrical measurements on stannic oxide were made in 1937 by BAUER (24). These samples were polycrystalline thin films prepared by the thermal oxidation of tin evaporated on a quartz plate. The specific conductivities of these films were between 10^{-4} and 34 $ohm^{-1}cm^{-1}$ and mobility varied between 0.9 and 6.6 cm^2 $volt^{-1}$ sec^{-1}.

Different workers such as AITCHESON (2), BURKETT (25) and HOLLAND (26) gave other techniques of preparing thin films. Improvement and stability in thin films were brought by MOCHEL (27) who pointed that by adding antimony to these films gave a higher and positive temperature coefficient of resistivity.

Two papers by ISHIGURO (13) and IMAI (1) report electrical and optical measurements on both undoped and antimony doped stannic oxide films. ARAI (29) interpreted these results and his own by proposing a tentative energy band scheme, and concluded that the predominant scattering mechanism at room temperature even in undoped films was that of ionized impurity.

MILOSLAVSKII and LYASHENKO (30) and (31) found that the depth of the energy level associated with each antimony ion in their thin films is at 0.15 ev. Further infrared work (32) showed that electron effective mass varies with donor concentration. An extension of his work (33) in the visible and ultraviolet region showed for energies $h\nu > 4$ ev that absorption is due to direct permitted interband transitions.

KOCH (12, 35, 36) found from his electrical and optical measurements on thin films that at room temperature scattering by longitudinal optical modes is the dominant

scattering mechanism.

TIGANE (37) used an Electron Microscope to study the causes of decrease in conductivity in stannic oxide films.

GOLOVCENCO (38) (39) produced stannic oxide films by the pyrolysis of $SnCl_2 \cdot 2H_2O$ and $SnCl_4 \cdot 5H_2O$ in addition with $B(OH)_3$ and studied their electrical conductivity as well as the boron influence on these films.

The most recent method for the preparation of thin films is by IACHIMOWSKI (40), who obtained the thin films by sputtering from a cathode covered with high purity tin.

(b) Polycrystalline Samples

LOCH (41) prepared samples of stannic oxide by compressing SnO_2 powder with various proportions of antimony to act as a donor impurity. The electrical conductivity and seebeck coefficient were measured in vacuum. The mobility of these specimens varied in the range 10 - 12 cm^2 $volt^{-1}$ sec^{-1} and it did not change with temperature over the range 100 - 800°C. This small value of mobility was interpreted as the effect of grain boundaries and other imperfections in the samples.

VAN DALL (9) had obtained some polycrystalline stannic oxide samples of high purity from sintered pellets. These samples were prepared at about 900°C, via an exothermic reaction,

much below the temperatures for crystal growth. The impurity content was correspondingly lower, by an order of magnitude. The results of measurement on these samples are given in Fig.(111.2, 111.3).

(c) Natural Single Crystals

KOHNKE (42) measured the electrical and optical properties of good natural crystals. The activation energy for intrinsic conduction above $800^{o}K$ was 3.05 ev; and the energy gaps as obtained from optical absorption and photoconductivity measurements were 3.54 and 3.44 ev respectively. The Hall mobilities in different crystals at room temperature varied from 7 to 315 cm^{2} $volt^{-1}$ sec^{-1} and increased with increasing carrier concentrations.

(d) Synthetic Single Crystals

Different methods of crystal growth have been mentioned in Chapter 2.

MARLEY and DOCKERTY (43) had reported the results on several undoped and antimony doped crystals grown by Helium flow method. NAGASAWA (44) published the measurements made on single crystals which were grown by the hydrolysis of stannic chloride. VAN DALL (9) had explained the results of the measurements which were made on several single crystalline and

polycrystalline tin oxide samples.

A brief survey of the results of these workers, as well as others, on conductivity, carrier concentration and mobility, is given in Fig.(111.1 to 111.4).

Key to Fig. 111.1 to 111.4

	Author	Material	Reference
————	Koch	Thin films	12
— — o — —	Imai	do	1
A	Arai	do	29
I	Ishiguro	do	13
o o o o o	Van der Maesen and Witmer	do	46
— — — △ — —	Van Dall	Single Crystal Fig.(111.1)	9
— — — △ — —	Van Dall	Polycrystal Fig.(111.2)	9
— · · — · · — · · —	Kohnke	Single Crystal	42
— — — + — — — +	Nagasawa	do	44
— — — o — — —	Marley and Dockerty	do	43
— — — □ — — —	Morgan	do	5

FIG III·1

Temperature variation of mobility of electrons in SnO_2 according to various workers

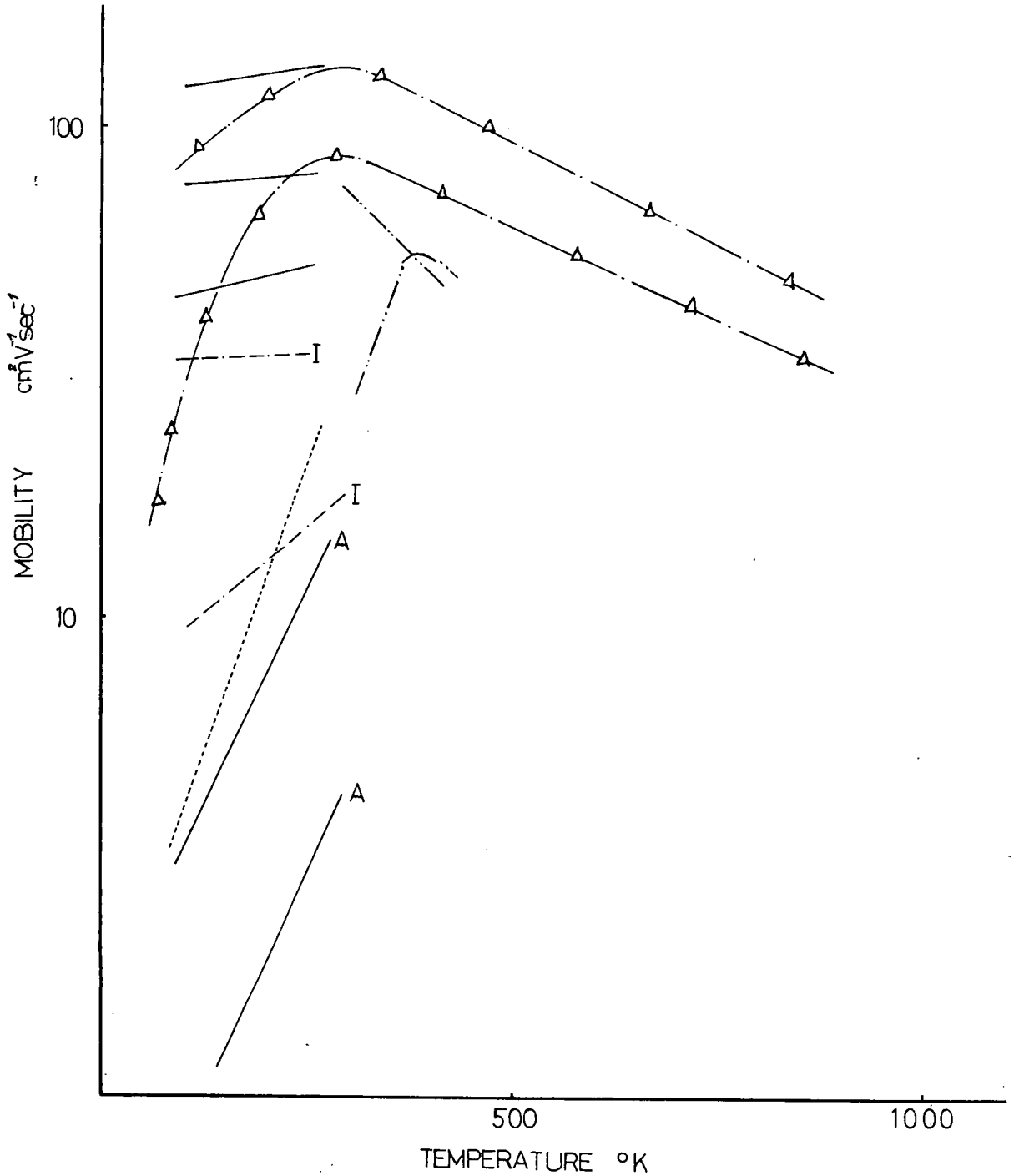

FIG 111.2

Temperature variation of mobility of electrons in SnO_2 according to various workers

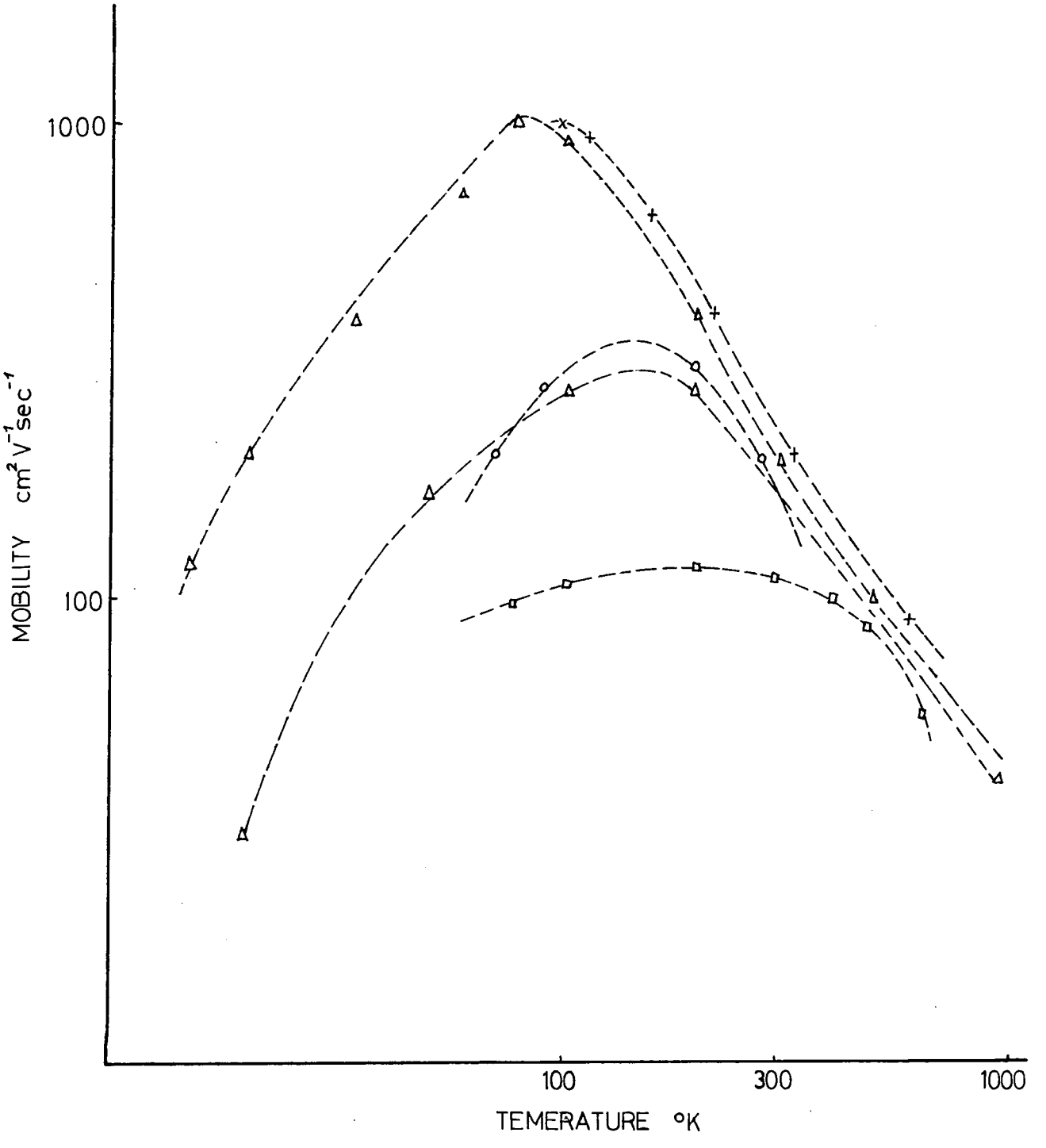

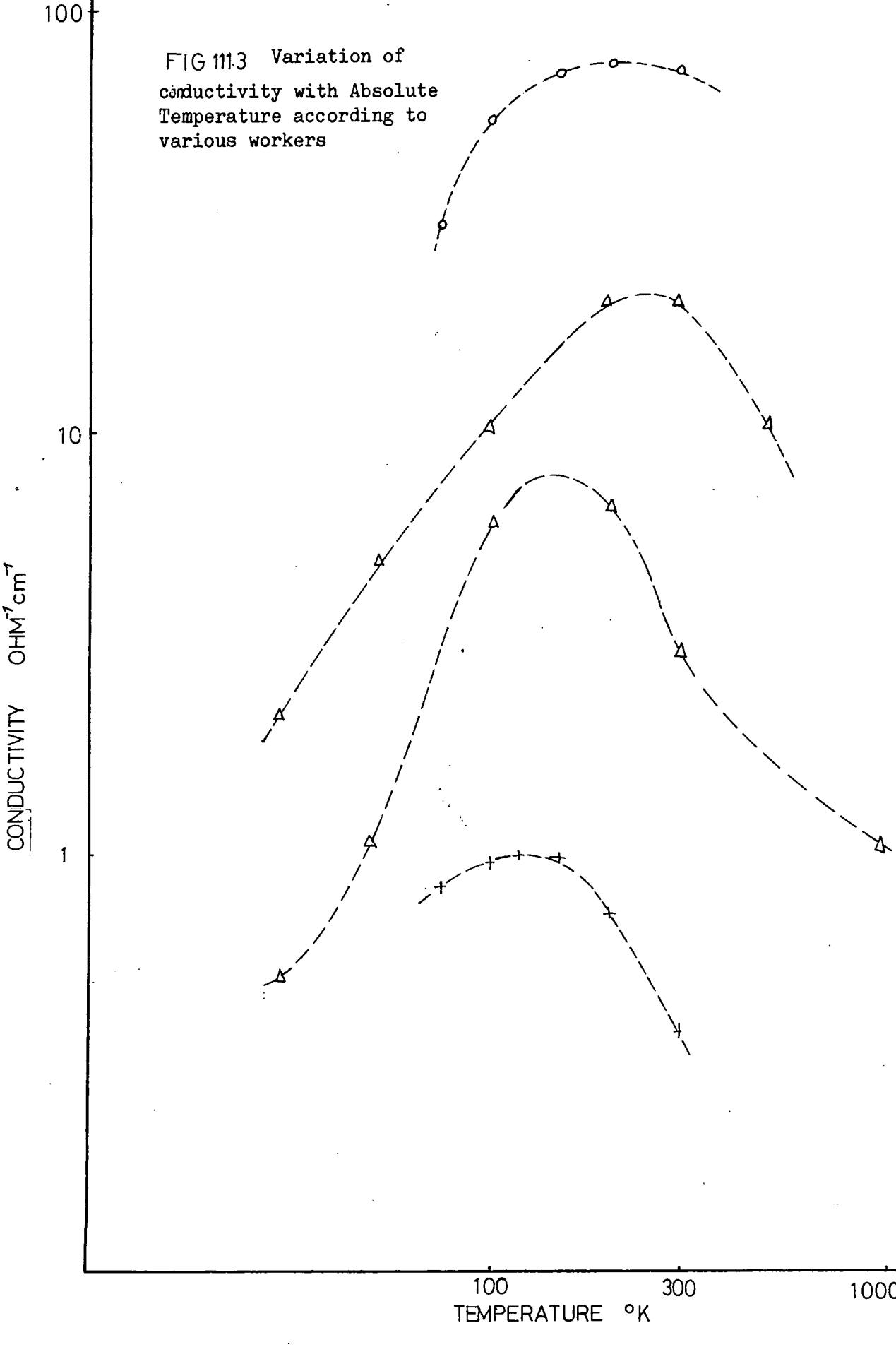

FIG 111.3 Variation of conductivity with Absolute Temperature according to various workers

FIG 111.4

Temperature variation of carrier concentrations according to various workers

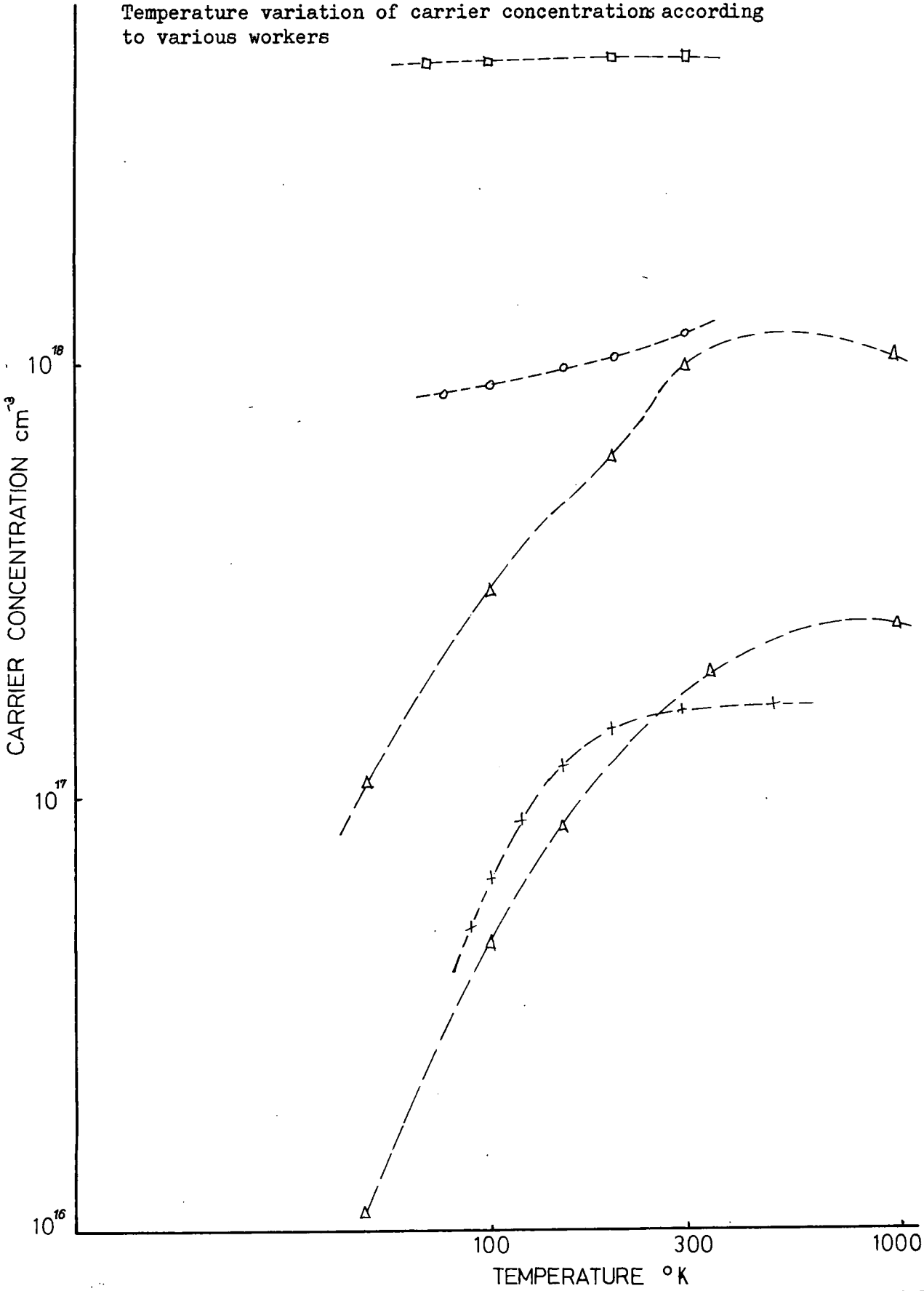

Section 3 Variation of Mobility and Conductivity with Temperature

(a) Marley and Dockerty

The Hall mobility and electrical conductivity had been measured Fig.(111.2, 111.3) on single crystals of n type SnO_2 between 80°K and 900°K. At low temperature the Hall mobility was found to decrease with decreasing donor concentrations and it was interpreted in terms of combined ionized scattering and impurity band conduction.

The mobility above 300°K was analyzed by considering polar optical modes of vibration as being the dominant scattering mechanism. Values of the donor ionization energy were found to decrease with increasing donor concentration and at infinite dilution it was found to be 0.15 ev.

(b) Nagasawa

NAGASAWA (44) measured the Hall mobility and conductivity of one crystal between 90°K and 300°K. From the results Fig.(111.2 to 111.4) he concluded that mobility is predominantly governed by the acoustic mode lattice scattering with a further contribution due to optical phonons. A slight variation in carrier concentrations in this temperature range was found Fig.(111.4). The activation energy was of the order of 0.024 ev.

(c) Morgan

The electrical properties of antimony doped single crystals of stannic oxide had been studied between 77°K and 1100°K as shown in Fig.(111.2, 111.4). These were interpreted in terms of optical mode lattice scattering at the higher temperatures with an impurity scattering contribution below about 300°K.

(d) Van Daal

The electrical measurements on polycrystalline and single crystalline stannic oxide are shown in Fig. (111.1 to 111.4). The Hall mobility at room temperature in single crystals is about 100 cm^2 $volt^{-1}$ sec^{-1}, and it decreases at low temperature, while the polycrystalline samples showed a mobility around 200 cm^2 $volt^{-1}$ sec^{-1} at room temperature. An increase in mobility was observed up to liquid nitrogen temperature. The relatively low donor ionization energy is at most 0.01 ev.

From the measurement carried out for a wide range of temperature 4°K to 1600°K and optical reflection in Reststrahl region, it was concluded that polar optical modes with an average characteristic temperature of 1050°K dominate lattice scattering.

Section 4 Electron Effective Mass, Dielectric Constant, Magnetoresistance

(a) Electron Effective Mass

The electron effective mass of SnO_2 thin films had been measured by KOCH (35). A value of 0.17 m_o was deduced from the measurements of optical dispersion. KOHNKE (42) had deduced a value of 0.8 m_o in natural single crystals of stannic oxide.

NAGASAWA (44) had performed measurements of thermoelectric power at room temperature and obtained a value 0.35 m_o. These calculations were based on assuming the acoustic mode lattice scattering ($S = -\frac{1}{2}$). MARLEY and DOCKERTY (43) also carried the same measurement at room temperature and obtained a value between 0.12 m_o and 0.18 m_o, assuming ionized impurity scattering ($S = 3/2$).

MORGAN (5) found a value 0.16 m_o from his experiments for a wide range of temperature between 300°K to 1100°K. At 100°K the value with S = 3/2 (ionized impurity scattering) is 0.13 m_o, while $S = \frac{1}{2}$ gives 0.19 m_o. WRIGHT (45) pointed out that this value did not depart significantly from 0.16 m_o. He also pointed out that there was evidence of anisotropy in m_e

with values of 0.16 m_o perpendicular to c-axis and 0.11 m_o parallel to it.

LYASHENKO and MILOSLAVSKII (32) had taken account of the electron theory of impurity band (47) and reported a value of effective mass between 0.2 and 0.3 m_o. According to them the most reliable values for the effective mass is obtained when $N > 10^{20} cm^{-3}$.

VAN DAAL (9) assumed that polar scattering is the dominant process in SnO_2 so a value of 0.3 m_o was derived. These values were consistent with weak coupling theory. The value of α_c (the electron phonon coupling constant) is approximately one, implying that polaron effect can not be neglected. Intermediate coupling theory by LOW and PINES (34) which takes account of polaron effect leads to 0.24 m_o. VAN DAAL concluded that the value for m_e^* lies well within the range 0.2 - 0.3 m_o.

(b) Dielectric Constant

The static dielectric constant for different direction in crystal (parallel to c-axis and perpendicular to c-axis), according to Handbook of Chemistry and Physics (28) was 24 and 23.4.

VAN DAAL (9) from his optical reflection

measurements on single crystals of SnO_2 between 2 μ to 50 μ found that dielectric constant perpendicular to c-axis and parallel to c-axis has values about 9 and 15. These values were further confirmed by microwave measurements.

(c) Magnetoresistance

The magnetoresistance measurement on n-type SnO_2 had been performed by NAGASAWA (4). The magnetoresistance was found to be proportional to (magnetic field)^2 up to at least 15 KG (Fig. 111.5). Three types of specimen which were typically 0.5 x 0.5 x 4 mm in dimensions having length direction cut along [100] , [001] and [110] , respectively were prepared. Two terminal method was employed for the magnetoresistance measurements.

The measurements were carried out at room temperature, 77°K and 20°K, but only relative resistivity changes up to a few percent were observed in tranverse magnetoresistance at 77°K under the magnetic field of 15 KG.

The explanation of the results can be offered as follows. The directional magnetoresistance coefficients are defined as M_{hkl}^{mnp}, where subscript gives the direction of the current while superscript that of magnetic field. The coefficients

FIG 111.5

$\frac{\Delta\rho}{\rho_0} V_s \quad H^2$ in SnO_2 as measured by Nagasawa

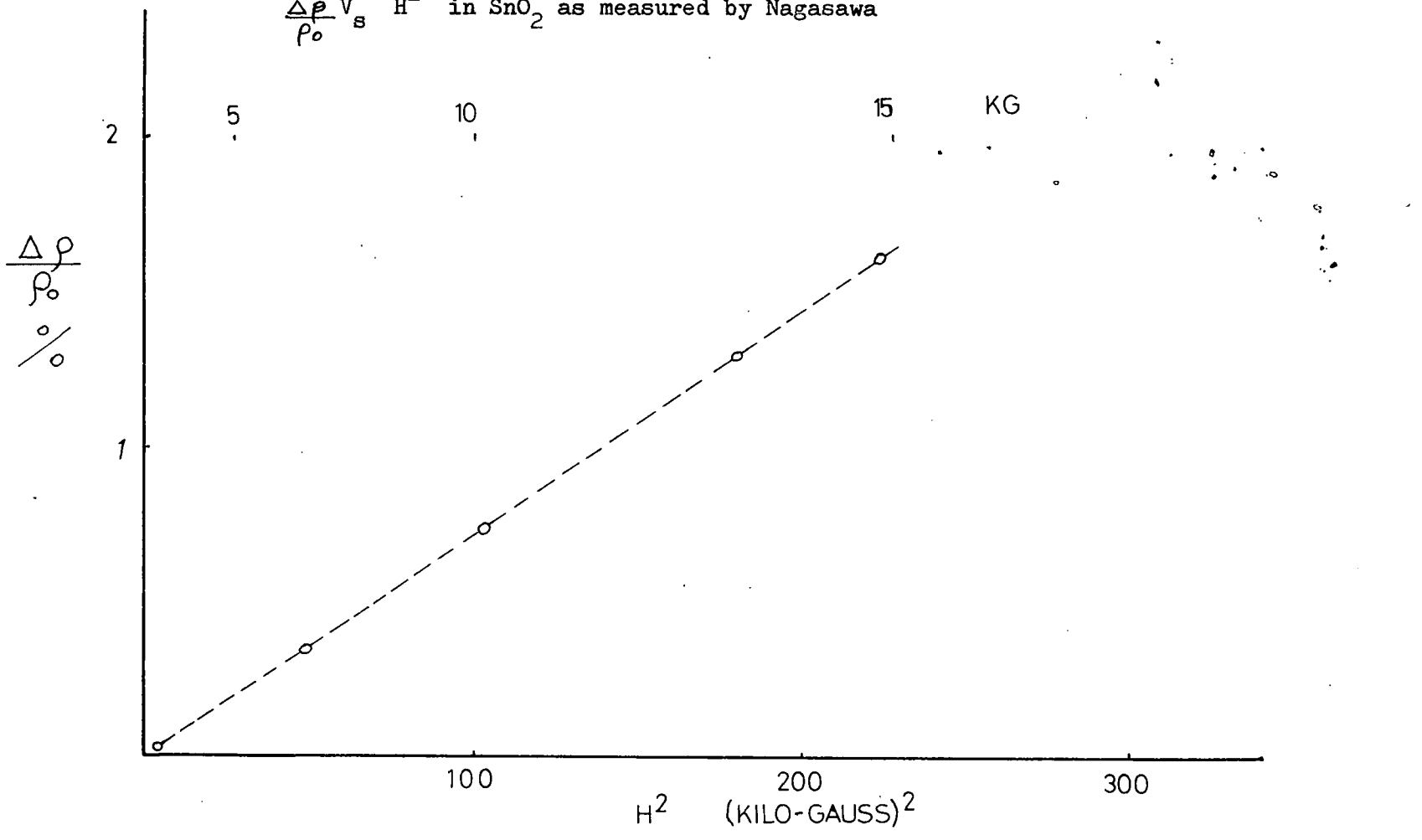

found from the measurements of magnetoresistance for a sample having current parallel to $[100]$, leading to the conclusions:-

(A) longitudinal magnetoresistance coefficient (minima) $M_{100}^{100} < M_{100}^{010}$ transverse magnetoresistance coefficient (Maxima)

(B) similarly Transverse Maxima $M_{100}^{010} > M_{1001}^{001}$ Longitudinal Minima

From the second sample, having current parallel to $[001]$, it appeared that:-

Longitudinal Magnetoresistance coefficient $M_{001}^{001} < M_{001}^{100}$ Transverse magnetoresistance coefficient maxima

From the observation of third crystal having current in $[110]$ direction the same result was obtained.

The above results were interpreted as an anisotropy in the crystal structure, that is, the direction 100 is no longer equivalent to $[001]$ in the crystals having the point group D_{4h} symmetry.

Furthermore it was assumed that an anisotropy is due to anisotropic scattering process, since anisotropy

factor is different from sample to sample. It was therefore difficult to estimate the effective mass ratio from the anisotropy factor obtianed by their investigations.

The value of magnetoresistance coefficient observed agrees well with that calculated assuming that an ionized impurity scattering process is dominant at this temperature(77°K)

CHAPTER 4

EXPERIMENTAL METHODS AND RESULTS

Section 1 Introduction

As described in Chapter 2 it was found possible to grow crystals of good quality and high purity. These were suitable for studying the intrinsic electrical and other related properties.

Materials for use in thermoelectric devices usually have high carrier densities $\backsim (10^{19}$ carriers/cm$^3)$, so antimony doped specimens with carrier densities $7.10^{18} - 7.10^{17}$/cm^3 were also studied.

A big amount of work was done on undoped reduced stannic oxide single crystals with the possibility of obtaining high mobility crystals, which have electron densities in the range $1.3 \times 10^{18} - 6.5 \times 10^{16}$/cm^3. The electrical conductivity and Hall coefficient were measured between room temperature and 77°K while magnetoresistance measurement was done at 77°K on one specimen.

Two probe conductivity measurements were also carried out on undoped stannic oxide rods between 700-1300°K.

Section 2 (a) Sample Holder

The sample holder used for Hall effect, conductivity and magnetoresistance measurements is shown in Fig. (4.1). The base was machined from a piece of Sindanyo which is an excellent thermal and electrical insulator. On the top of the holder a perspex sheet of 2.5 x 4.75 cm was fixed which holds the crystal. Five holes were drilled through the sheet. They were held in contact by phosphor bronze strips tensioned by screws.

A non-inductive heater was provided on the back of the holder. Temperatures were measured by a copper constantan thermocouple embedded in a thick copper block which lay between the holder and the sample. It was assumed that this gave the temperature of the sample. A thin mica sheet separated the contacts of the perspex from the thermocouple and the copper block.

(b) Indium Contact

Silver contacts were not found very satisfactory for the electrical measurement as they were noisy. An alternative method (14) for contact preparation was also tried by applying an alloy of indium and gallium to the sample, but this

Fig 4.1 HALL EFFECT HOLDER AND CIRCUIT

a)

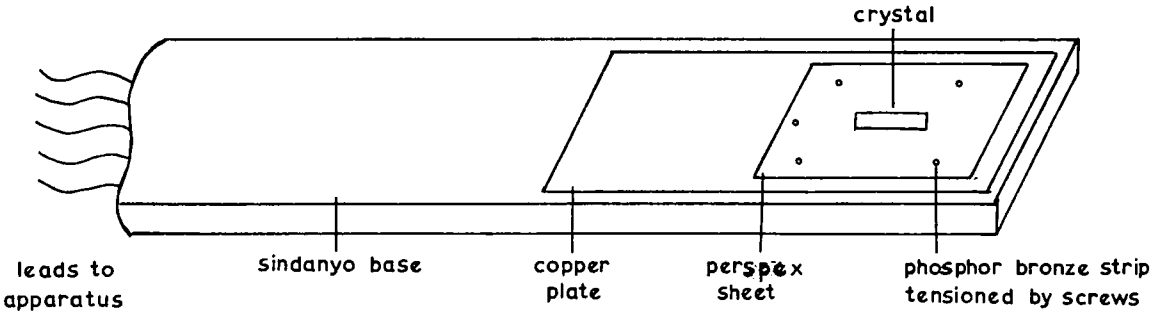

b)

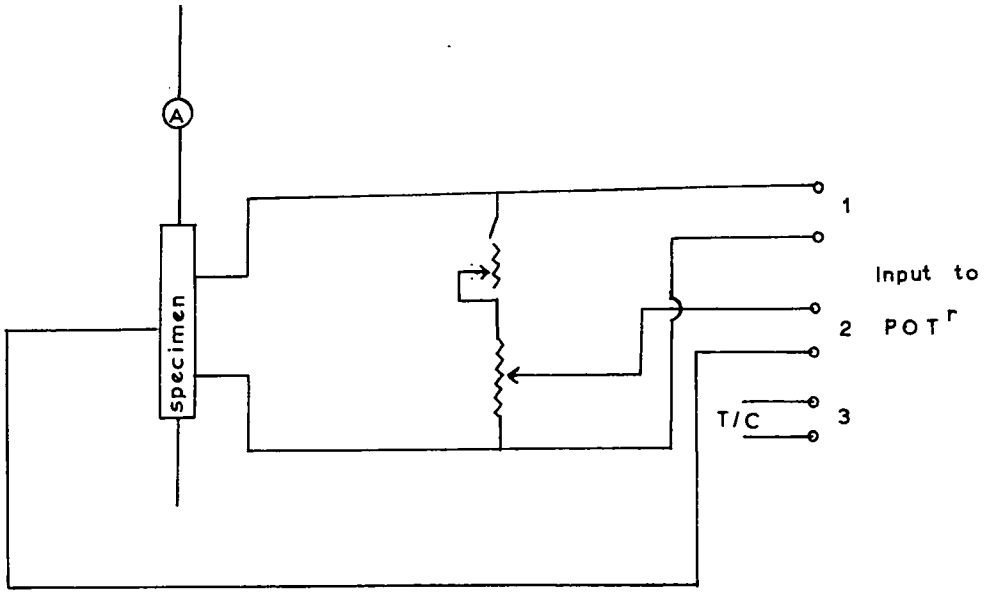

was abandoned in favour of the more successful indium evaporated contact method.

Edwards High Vacuum Unit was used for the preparation of indium contacts. First the rod crystals were cut and ground to the form of rectangular bars and then were etched by using a boiling solution of 47% hydriodic acid (HI) with a small quantity of hypophosphorous acid (H_3PO_2) added to remove excess of iodine.

Indium was outgassed and evaporated from a molybdenum strip. The crystal was mounted above the heater strip and in contact with a suitable aluminium mask.

A technique by WRIGHT (48) was found very successful here according to which the crystal has to be heated at about 160°C in vacuum after the indium evaporation so that diffusion of indium inside the crystal takes place.

After the contact preparation the crystal was attached on the perspex sheet with the durofix. Silver dag was used to make electrical connection between evaporated indium and phosphor bronze strips.

(c) The Magnet

The magnet was a medium sized air cooled

electromagnet which provided an induction of 6 kilogauss at a pole gap of 5 cm working at 10 amperes and 120 volts D.C. The pole faces were 7 cm in diameter. A circuit of different variable resistances was used to control the current to the magnet. The magnet could be run for sufficient time to take all measurement without any noticeable drop in induction.

(d) Conductivity Measurement

Conductivity measurements were made with the four probe technique which has been used by MITOFF (49). PhillipsD.C. microvoltmeter G.M. 6020 was used for this purpose. This could measure voltages down to 10 μV on its low impedance range of 1 megohm and up to 10 volts on its high range of 100 megohm. The input impedances were much higher than any sample impedance measured.

Readings of conductivity or Hall coefficient at liquid nitrogen and other low temperature regions were taken using a cryostat. The voltages produced by the thermocouple were measured with a potentiometer. The cold junction was immersed in melting ice and readings were taken with the temperature of the specimen increasing from 77^{o}K to room temperature.

(e) Hall Effect Measurement

A five probe method was adopted for the Hall

effect measurements of low resistivity crystals whether doped or undoped (Fig. 4.1). Current to the crystal was supplied through a stabilized power source, and could be adjusted accurately by means of a cascaded potentiometer and a milliameter.

The accuracy of the milliameter could be checked by measuring the voltage developed across a 10 ohm standard resistance. Hall voltage was measured by a Tinsely potentiometer type 33876 capable of measuring division of one microvolt.

The Hall coefficient was calculated from the formula

$$R = \frac{t}{HI} \times V_H \times 10^8 \quad cm^3/coulomb$$

During the measurement, the current and magnetic field were reversed so that errors due to other effects could be eliminated. Corrections to the measured Hall voltage due to the contact shorting (50) were applied if the sample geometry required it.

Section 3 Heat Treatment on Undoped Crystals

The following experiment has been performed in four different conditions on undoped crystals.

(a) Presence of Oxygen

(b) Presence of Argon with Current passing through crystal

(c) Heating in Air at low pressure, with current passing through crystal

(d) Heating in Air at low pressure or reduction.

(a) Oxygen

Two probe conductivity measurements were carried out on an undoped stannic oxide rod between 700 and 1300°K. Platinum paste with platinum wire was used for the contact. Platinum-Rhodium was used as thermocouple. Oxygen at a rate 25 cc/minute was passed over the crystal, while the crystal was heated for about 25 hours at 1300°K.

Measurements of conductivity were done before and after the heat treatment. No variation in conductivity outside experimental error was found. An activation energy of 3.84 ev with eqn.

$$\sigma = B \exp^{(-E_{act}/2kT)}$$

was calculated in this temperature range (Fig. 4.2).

(b) Argon

The same experiment as above was carried

Fig 4.2 Temperature variation of resistivity of high resistivity SnO_2 crystal

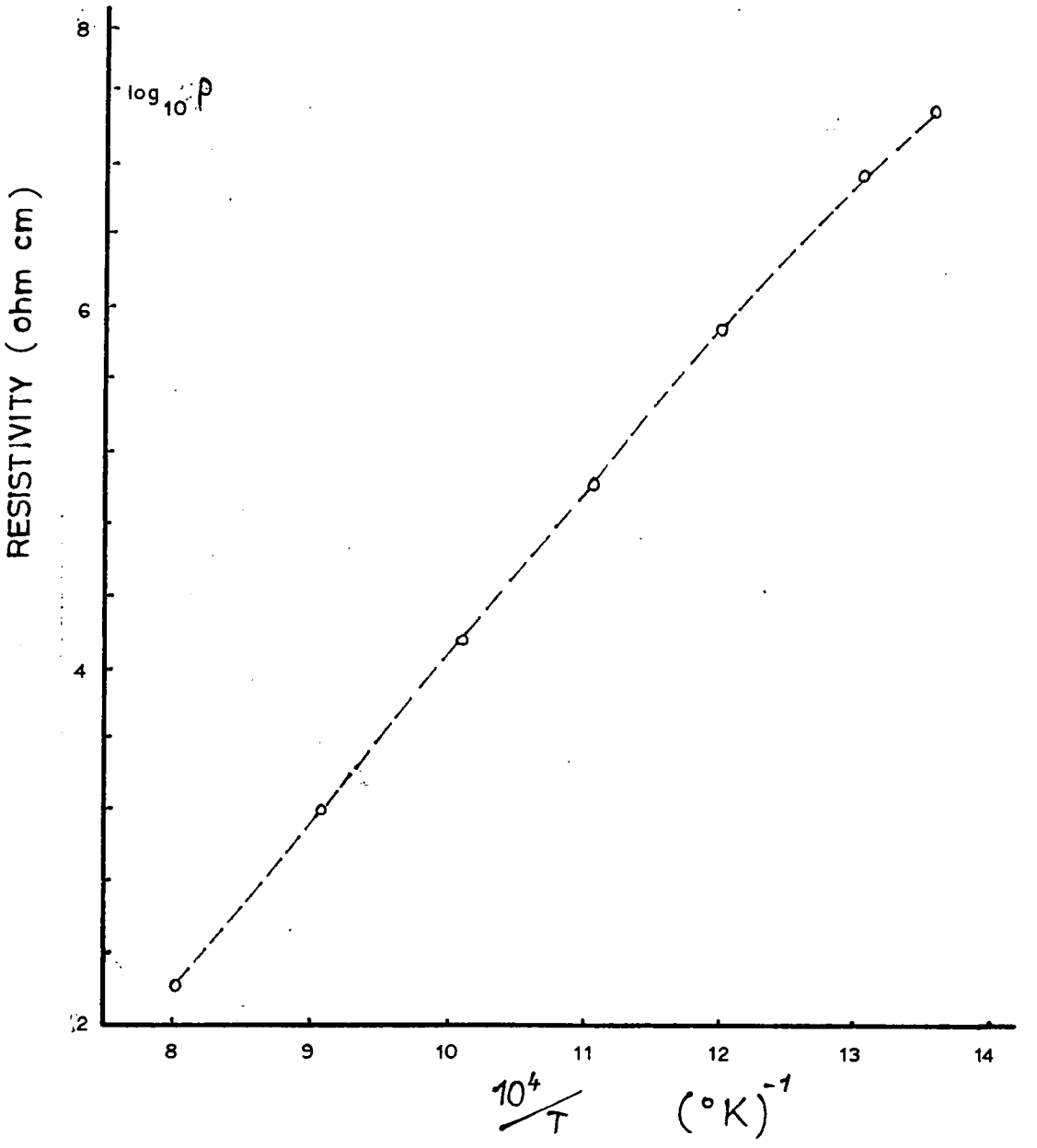

out in the presence of 40 cc/minute of Argon. A current density of ∽ 1 amp/sq.cm was passed through a crystal of high purity while the crystal was heated at 1200°K for twenty four hours. No change in colour of the crystal was observed, and there was no change in conductivity. The crystal was also heated at 1200°K in the presence of Argon without the current passing and it showed no change in colour or conductivity.

(c) Heating in Air at Low Pressure with Current passing through Crystal

An attempt to observe the effect on conductivity due to passing current was also made on two different kinds of crystal. A holder Fig. (42a) was made of baked pyrophyllite with platinum contacts. The crystal was fixed between the platinum contacts with the help of a tensioning screw. Another screw on the top of the holder kept the first screw in position against small vibrations.

The holder was placed in a small furnace which was placed in the vacuum unit. At a pressure of 10^{-4} mm of Hg, current of 100 mA was passed through a pink crystal grown by method 'A' (see crystal growth) for about four hours at a temperature of 430°C. No change in conductivity due to this treatment was found, however the crystal became less pink in colour.

Fig 4.2 a High temperature holder for the current passing experiment

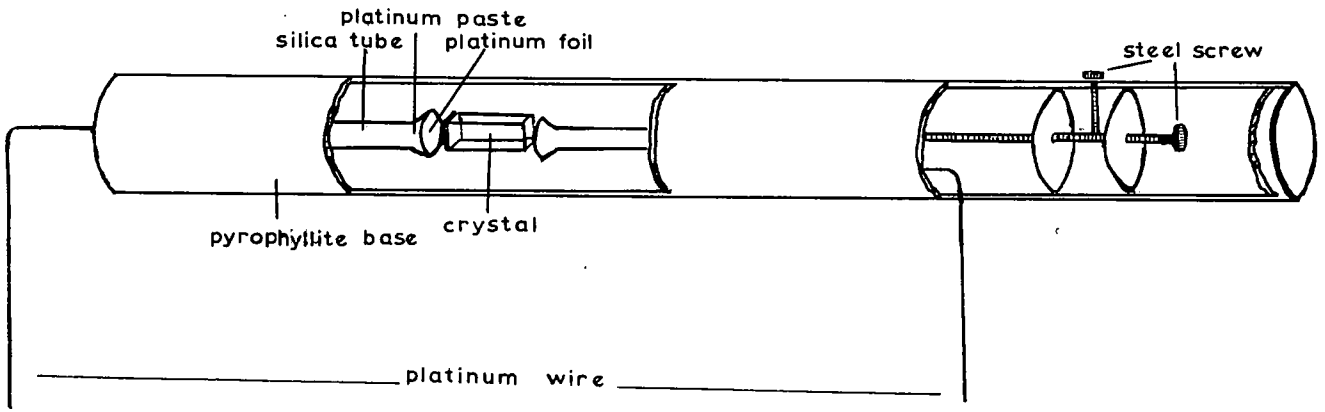

Keeping all conditions the same another transparent crystal grown by method 'C' was also treated. The conductivity increased by two order of magnitude, while the crystal remained transparent.

It is important to mention here that no change in conductivity was observed when crystals grown by any of the methods were reduced at a temperature of $430^{\circ}C$ and a pressure 10^{-4}mm of Hg without the passing of current.

(d) Heating in Air at Low Pressure

A small Kanthal wound furnace was mounted inside the bell jar of an Edward evaporating unit. Typically crystals were heated for five hours at a pressure of 5×10^{-2}mm of Hg at $850^{\circ}C$. Seven crystals were selected for detailed examination, as described below. Crystal 1 grew in region 1, crystal growth 'A', 2 to 7 were grown by method 'C' (see crystal growth).

Specimen 1 : Heated for five hours at $850^{\circ}C$ while the air pressure was 5×10^{-2}mm of Hg.

Specimen 2 : Substantially the same heat treatment was carried out with a decrease in air pressure to 10^{-4}mm of Hg.

Specimen 3 : The temperature at which the crystals were maintained in previous runs was the highest which could be

obtained with the Eurotherm control system available for the Kanthal furnace. Specimen 3 was heated first at 700°C for the same length of time and a pressure of 5×10^{-2}mm of Hg. The initial conductivity was less than 10^{-16} ohm^{-1} cm^{-1}. No increase in conductivity was observed following this treatment, nor after similar treatment at 500°C, 600°C respectively.

However, heating at 700°C increased the conductivity to 10^{-5} ohm^{-1} cm^{-1}. The subsequent reheating at 850°C caused the conductivity to decrease to 10^{-6} ohm^{-1} cm^{-1}.

On heating the crystal in air at 1000°C for two hours using the crystal growth furnace, the crystal developed a reddish colour, which subsequently disappeared when the crystal was again heated in air at low pressure. However no increase in conductivity was observed.

Specimens 4, 5, 6, 7.: Heat treatment at 850°C for times between one and three hours at about 10^{-4}mm of Hg changed the conductivity by six orders of magnitude.

Section 4 (a) Conductivity and Mobility Results on Doped Crystals

The conductivity and Hall coefficient measurements were made on antimony doped stannic oxide single

crystals 8, 9, 10, 11. Table (4.1) gives the room temperature values of the electrical parameters of these crystals. Low temperature measurements were made on all of them. The results are plotted for crystal 8, whose behaviour was typical.

The conductivity at 77°K was half the value at room temperature, Fig. (4.3.), while an increase in Hall coefficient was observed at liquid air temperature Fig. 4.6. The mobility variation is shown in Fig.(4.4). (Fig.(4.3), (4.4) also give results on undoped reduced samples, as discussed later).

Table 4.1.

Room Temperature Values of Electrical Parameter of Antimony Doped Stannic Oxide

Specimen	8	9	10	11
R (coulomb cm^{-3})	8.37	10.8	1.15	1.04
N (cm^{-3})	8.8×10^{17}	6.8×10^{17}	6.4×10^{18}	7.1×10^{18}
σ ($ohm^{-1} cm^{-1}$)	11.98	6.7	65.01	87.1
μ ($cm^2 volt^{-1} sec^{-1}$)	100	72.36	76.7	90.67
Length (mm)	6.3	8.6	5.82	6.54
Thickness (mm)	1.61	0.98	0.82	0.69
Width (mm)	1.30	1.8	1.42	1.76
Colour	Transparent		Slightly blue	

Fig 4.3

VARIATION OF ELECTRICAL CONDUCTIVITY WITH RECIPROCAL OF ABSOLUTE TEMPERATURE.

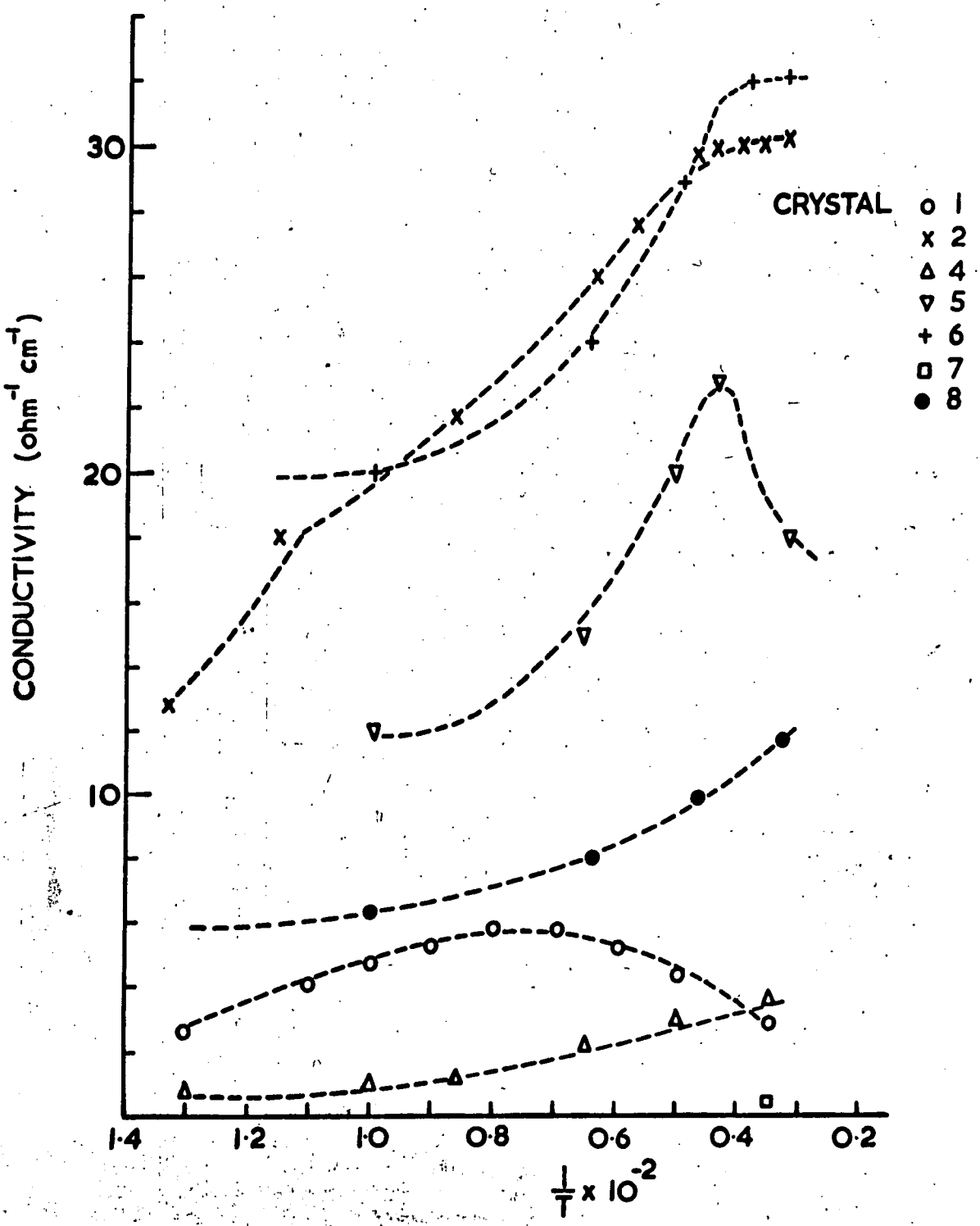

Fig 4.4

VARIATION OF HALL MOBILITY WITH ABSOLUTE TEMPERATURE

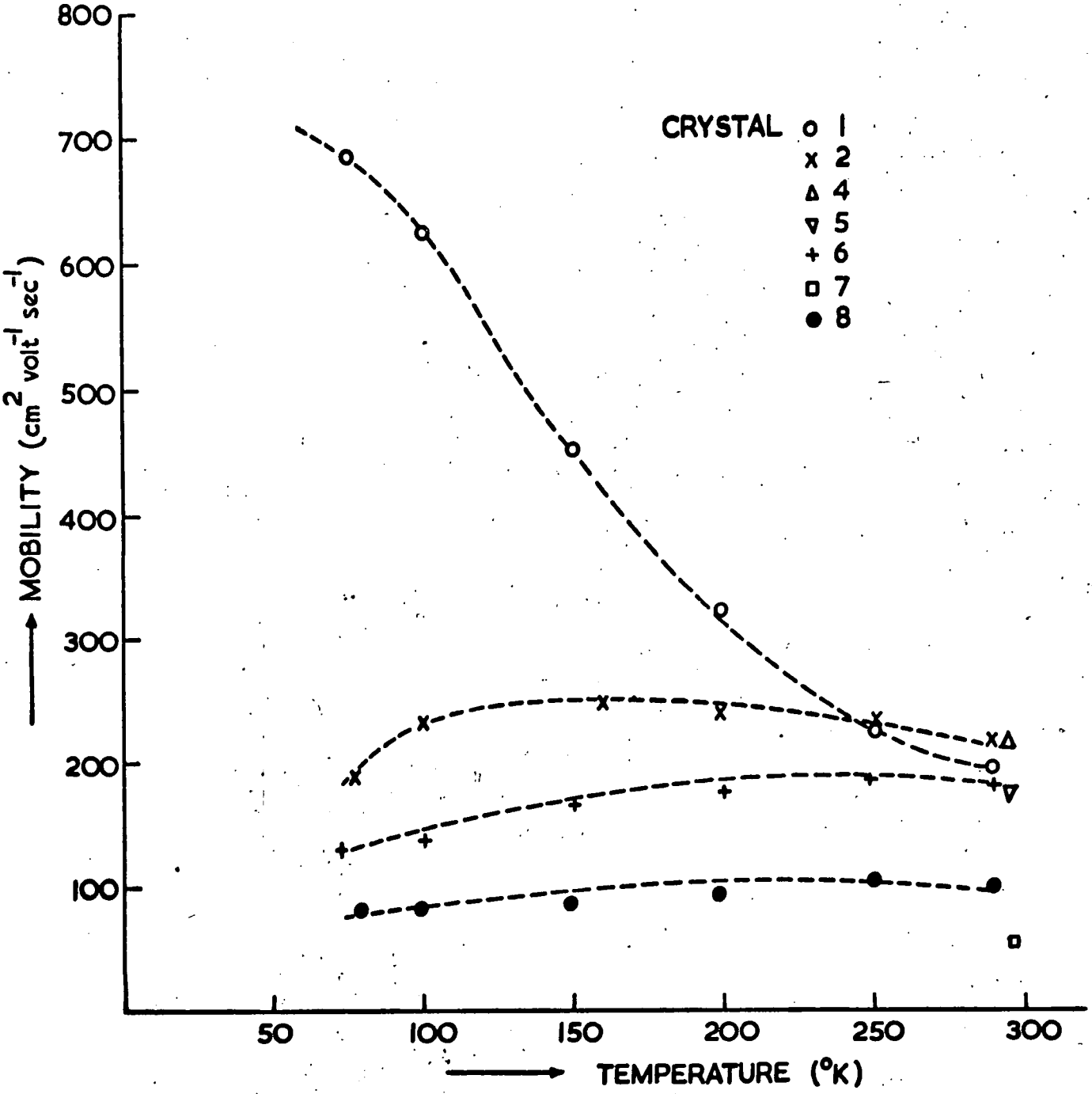

(b) Variation of Mobility of Undoped Reduced Crystals with Temperature

There was a big detectable change in the Hall coefficient of reduced specimens 1, 2 and 6 over the range of temperature measured, Fig.4.6. An increase in mobility of specimen 1 with charge carriers $10^{17}/cm^3$ was observed while specimens 2, 6 with charge carriers 10^{18}, $1.34 \times 10^{18}/cm^3$ respectively showed a decrease in mobility at liquid nitrogen temperature. The most accurate readings were obtained at room temperature and liquid air temperature where a constant temperature could be maintained while a number of readings were taken.

All the reduced undoped crystals were found to be non degenerate so a value of $3\pi/8$ was used for r.

The interpretation of the temperature variation of mobility is found in Chapter 6. The change in mobility and carrier concentration with temperature is shown in Fig. 4.4 and 4.6. Table 4.2 gives the room temperature value of the electrical parameters of all the reduced undoped specimens.

(c) Conductivity Variation with Temperature

Fig. (4.3) shows the variation of conductivity with temperature of reduced specimens 1, 2, 4, 5, 6. In the crystals 1, 5 there was an increase in conductivity up to $125^{o}K$,

TABLE 4.2

SPECIMEN	1	2	4	5	6	7
R (coulomb cm^{-3})	6.58×10	7.311	6.25×10	9.7	5.49	1.13×10^{2}
n ($_{conc}$ carrier/cm^3)	1.12×10^{17}	1×10^{18}	1×10^{17}	8×10^{17}	1.34×10^{18}	6.5×10^{16}
σ ($ohm^{-1} cm^{-1}$)	3.3	30.42	3.6	18	32.76	0.435
μ Mobility $cm^2 volt^{-1} sec^{-1}$	200	222	225	172	180	50
Length (mm)	6.46	5.22	4.422	4.2	5.68	7.42
Thickness (mm)	1.24	2.4	0.78	0.39	0.85	0.85
Width (mm)	1.96	1.02	2.54	3.78	2.37	1.66
Activation Energy	0.011ev	0.016ev			0.03ev	
Colour	A l l		T R A N S P A R E N T			

200°K respectively, while specimen 2, 4, 6 showed no such sign.

(d) Reversible Heat Treatment

The specimen 2 was recycled twice as follows; heating in air at 1000°C for two hours to make it non-conducting followed by reheating in the evacuated bell jar at 850°C for a few hours. Fig.(4.5) curve B_1 and B_2 showed the conductivity and mobility variation with temperature respectively.

With further reduction for five hours at the same temperature and pressure resulted an increase in conductivity and carrier concentration, while the mobility fell to half its value. Fig.(4.5) curve C_1 and C_2 shows the mobility and conductivity changes. Fig.(4.5) curve A shows the initial conductivity (reference) of the crystal.

The variation of carrier concentration with temperature for the above mentioned experiment is given in Fig.(4.6). The interpretation of above experiment is mentioned in Chapter 6.

(e) Grinding Experiment

The heat treatment at low pressure during which large changes in the conductivity occur takes only a few hours. So the following experiment was performed. A crystal from Nagasawa Run 4 (undoped reduced) was ground on two faces and the

Fig 4.5 Electrical results for reduced sample No.2.

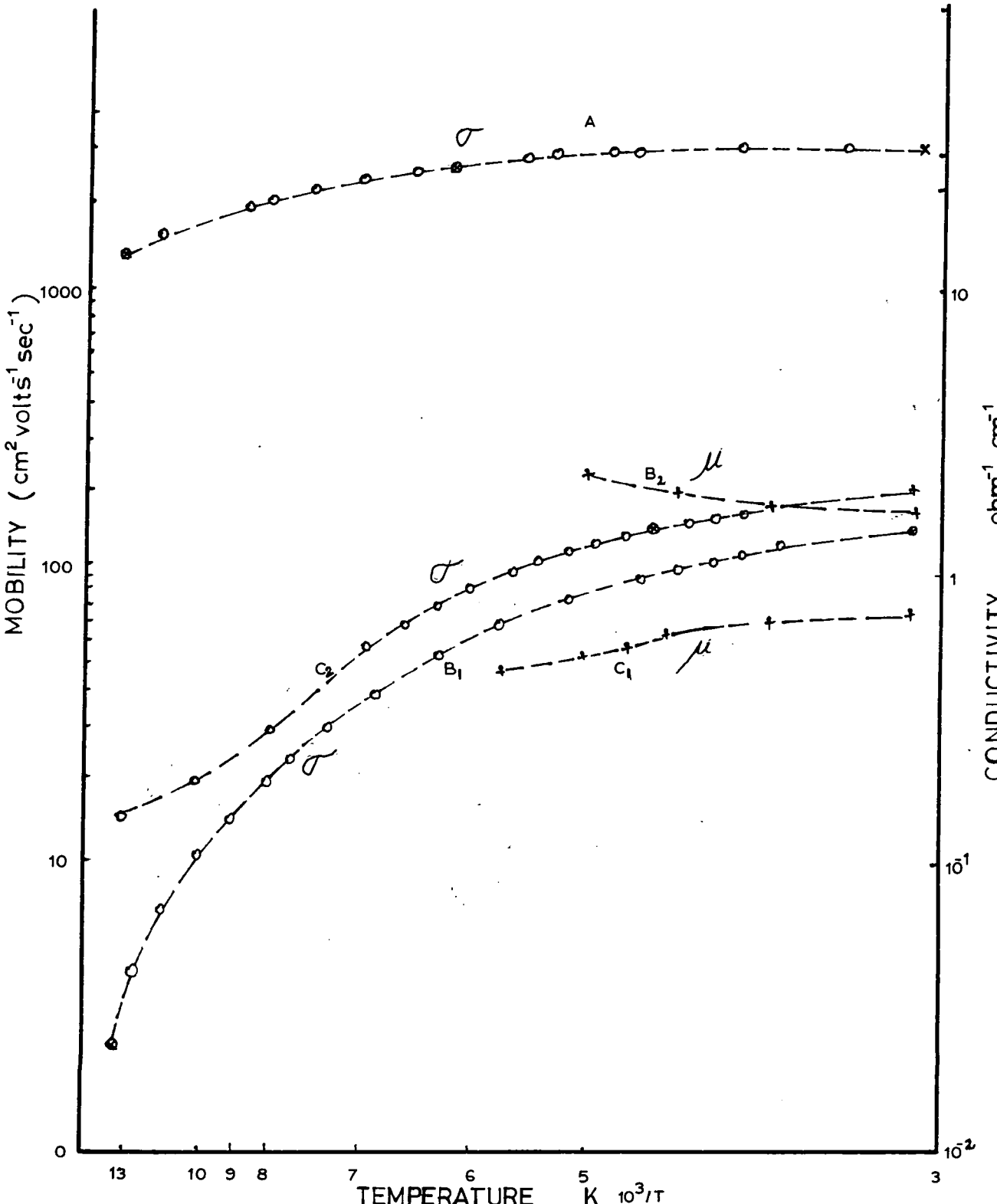

Fig 4.6 Temperature variation of carrier concentrations in reduced undoped crystals and antimony doped crystal

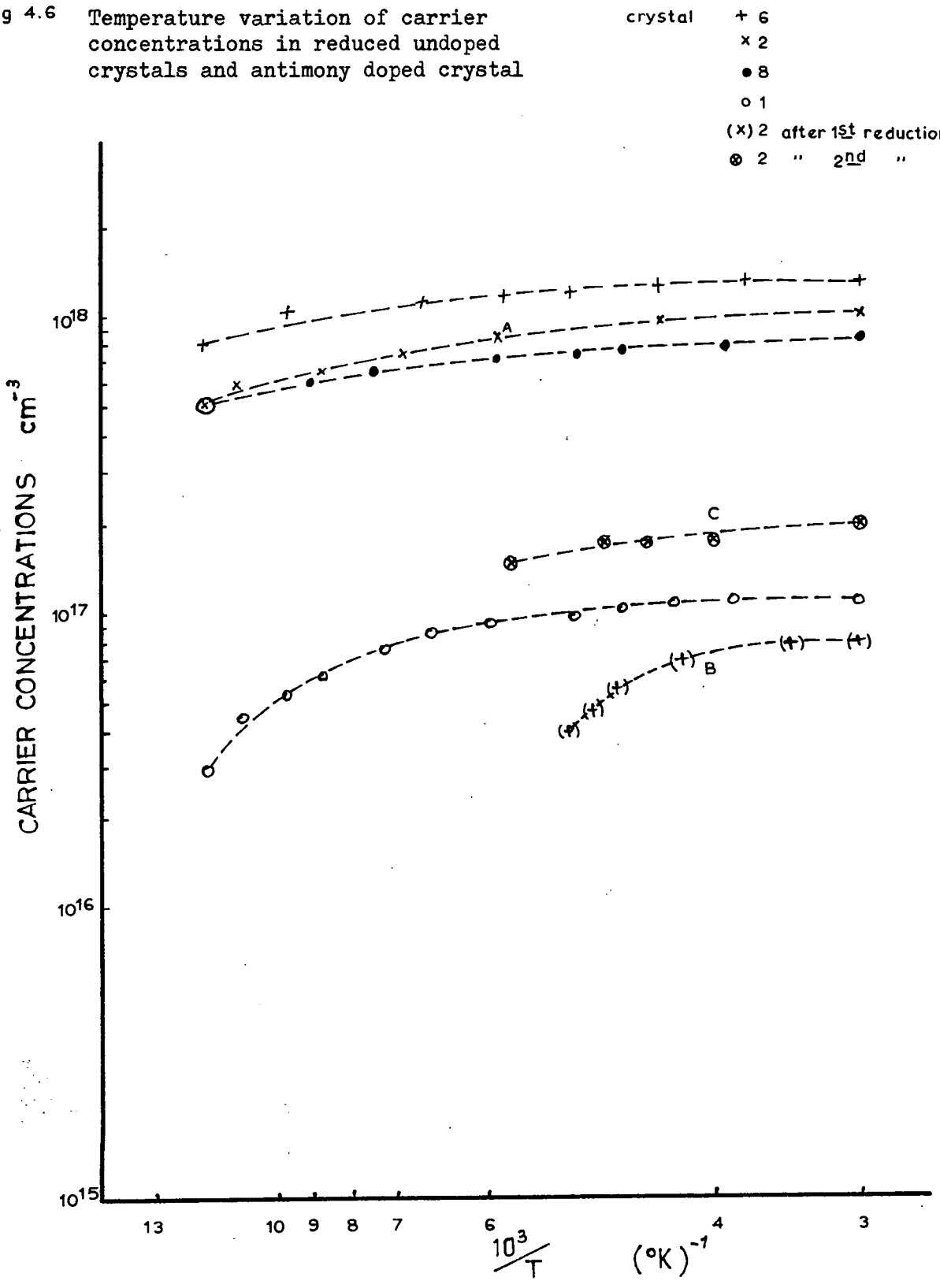

Fig 4.7 Conductivity variation with thickness in reduced undoped single crystal of SnO_2

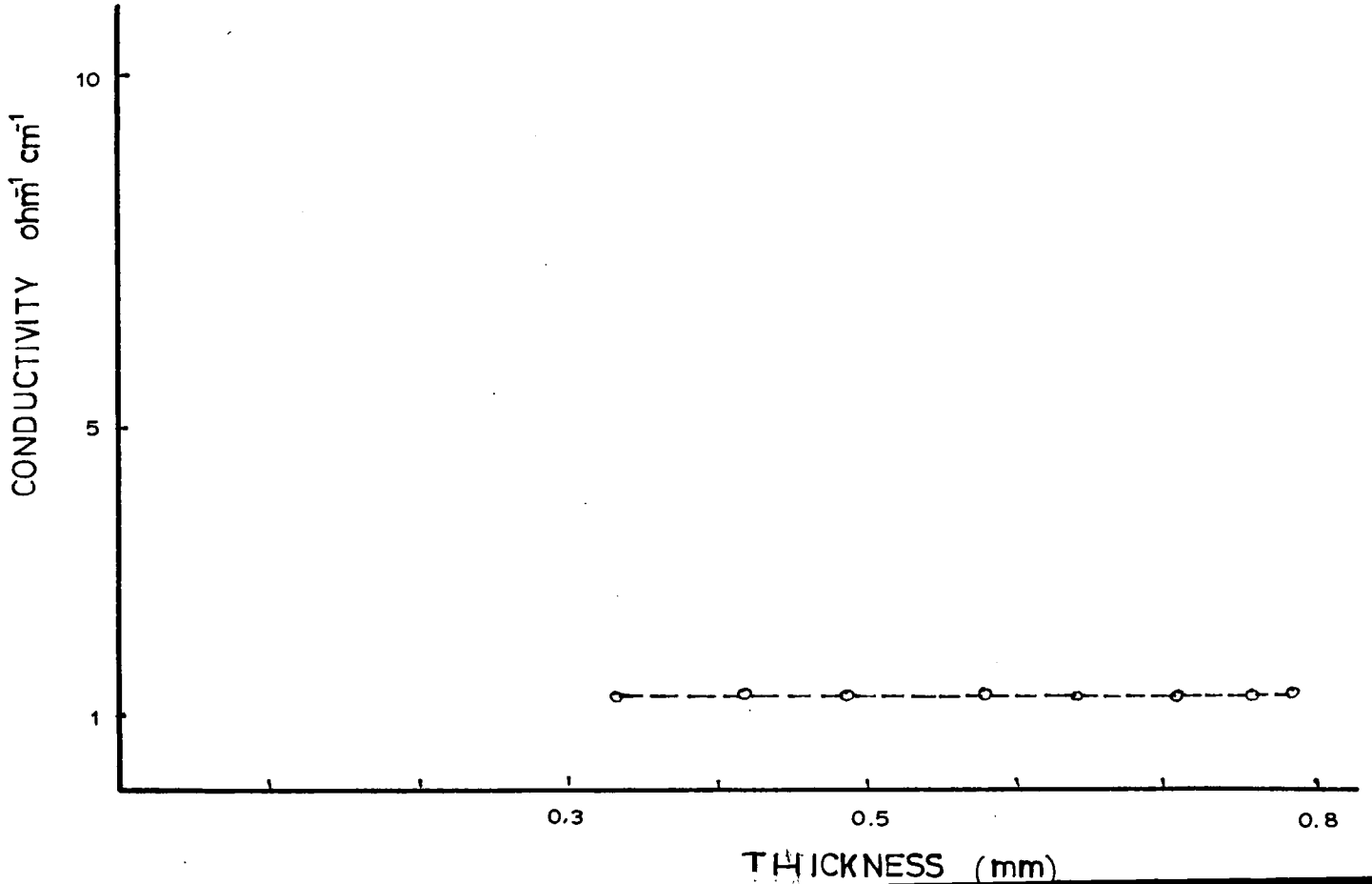

conductivity was measured at various stages in the grinding process. The thickness measurement was made with a sensitive micrometer. The scatter of the points in Fig.4.7 show only a 10% variation in conductivity with thickness which can be an experimental error.

(f) Magnetoresistance Measurement

The magnetoresistance was calculated from the change in resistance with magnetic field

$$\frac{\Delta P}{P_o} = \frac{P_H - P_o}{P_o} = \frac{V_H - V_o}{V_o}$$

where V_H and V_o are the voltages across the conductivity probes with and without the magnetic field respectively.

The change in resistance with magnetic field is known to increase with mobility. In view of the result shown in Fig.4.4 it was decided to make measurement on specimen 1 at liquid nitrogen temperature.

Potential measurements were made using a potentiometer and a galvanometer capable of measuring with one scale division equivalent to one microvolt. Sample current densities were kept constant to better than 1 part in 10^3 through a separate potentiometer system monitoring across a 1 ohm standard

resistance.

The possibility of the shorting of the Hall field, which increases the magnetoresistance (51) was avoided by making the distance between the conductivity probes very small in comparison to the length of the crystal.

Any thermoelectric voltage could be eliminated by reversing the current and taking the mean of the two readings. Magnetoresistivity measurements were made for magnetic field up to 15 Kilogauss at 77°K.

The magnetoresistance was found proportional to the square of the magnetic field up to at least 15 KG (Fig.4.9).

The variation of magnetoresistance with the angle θ between current and magnetic field for specimen 1 was determined at 77°K (Fig.4.10). The current was passing parallel to [101], while magnetic field in [010] swept to [0$\bar{1}$0]. Since all the measurements were performed in the transverse direction some work is required in longitudinal direction.

(g) Back Reflection Laue Photograph

Back reflection Laue photographs were used to discover the orientation of the crystals. The reference was normal to the large face, a mirror symmetry was obtained. Then

Fig 4.8

a)

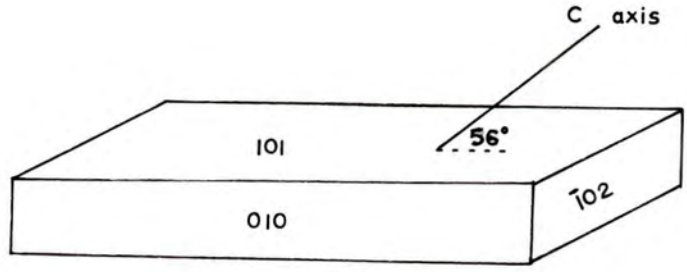

The direction of the C-axis in sample No.1

b)

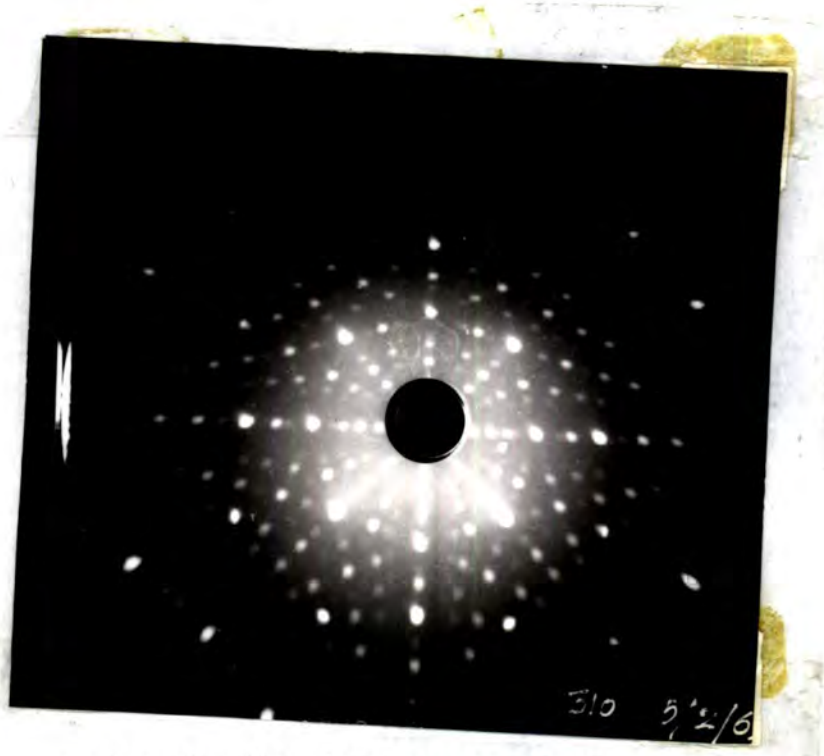

Back reflection Laue photograph of sample No.1 in the [001] direction

Fig 4.9

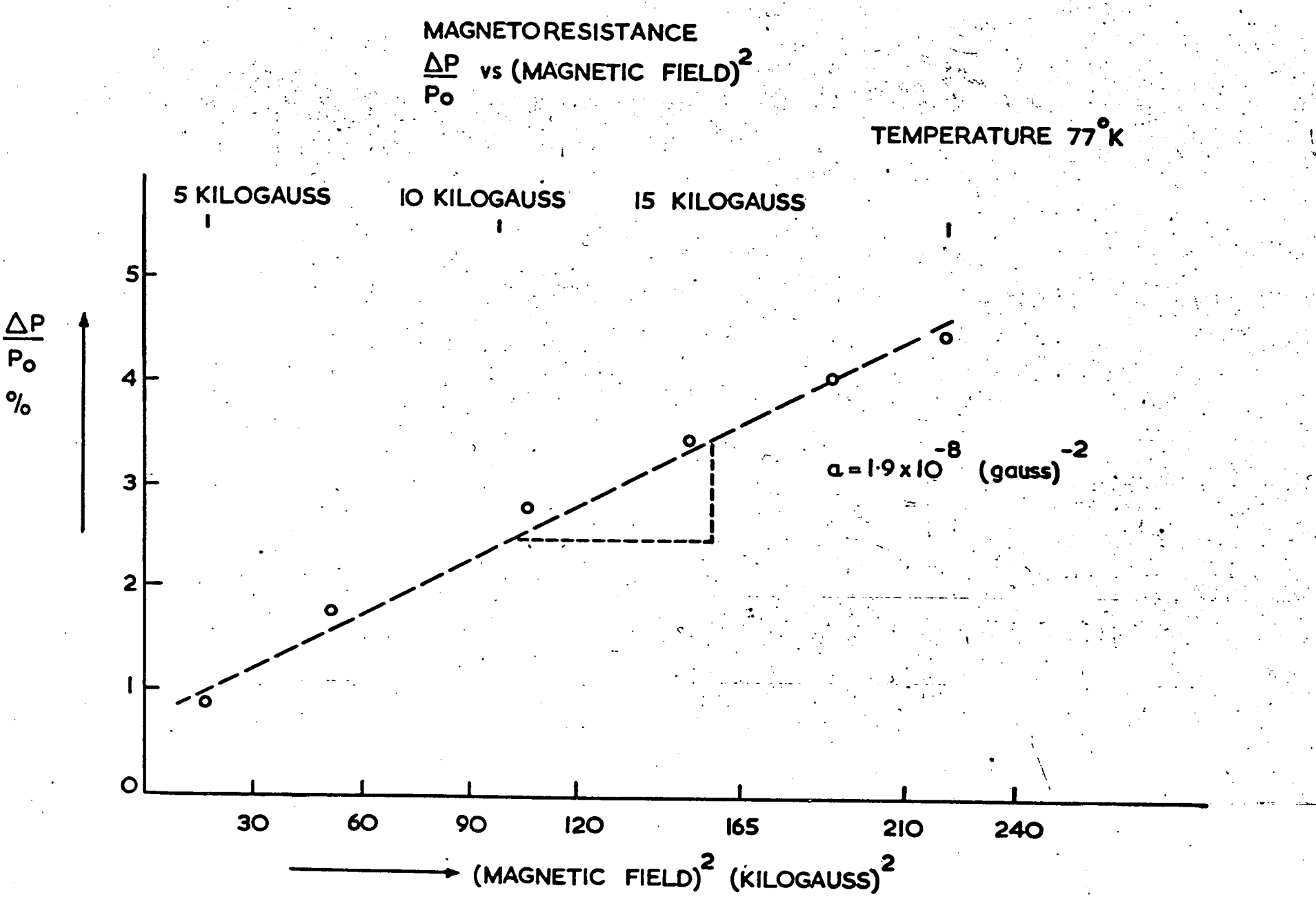
MAGNETORESISTANCE
ΔP/Po vs (MAGNETIC FIELD)²
TEMPERATURE 77°K
5 KILOGAUSS
10 KILOGAUSS
15 KILOGAUSS
ΔP/Po %
0
1
2
3
4
5
a = 1·9 x 10⁻⁸ (gauss)⁻²
30
60
90
120
165
210
240
(MAGNETIC FIELD)² (KILOGAUSS)²

Fig 4.10

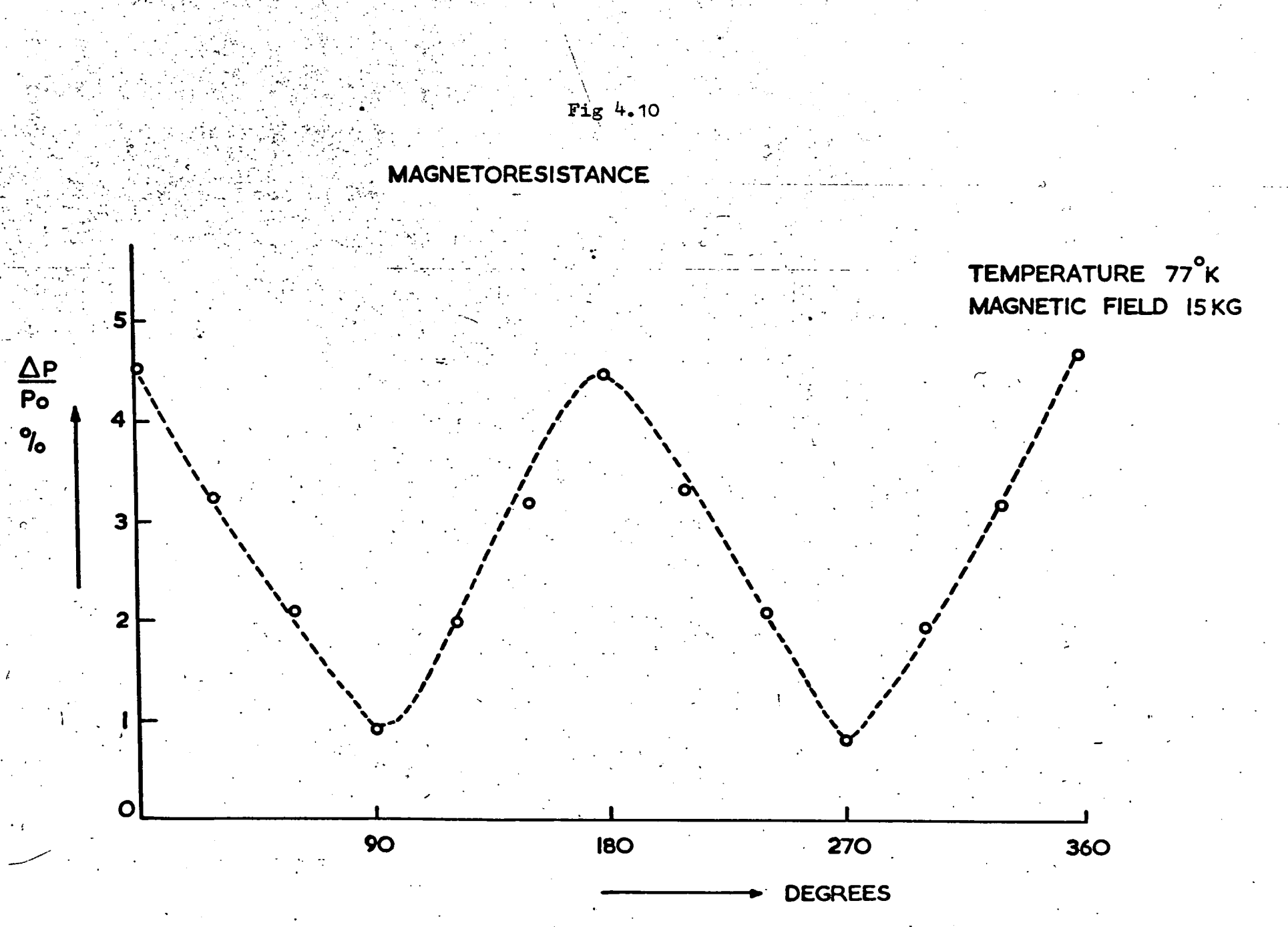
MAGNETORESISTANCE
TEMPERATURE 77°K
MAGNETIC FIELD 15 KG
ΔP/Po %
5
4
3
2
1
0
90
180
270
360
DEGREES

looking at the crystal model, mirror symmetry should be observed in the [101] plane. The C-axis could then be calculated as cutting the [101] plane at 56°, and lying in the 010 plane. This was confirmed by rotating the crystal 34° and taking a further back reflection photograph. The photograph taken with the crystal 3 cm away from the photographic plate in [001] direction, is shown in Fig.(4.8.b).

CHAPTER 5

OPTICAL PROPERTIES OF STANNIC OXIDE CRYSTAL

Section 1 Introduction

There is little information one can get in literature about optical absorption of the reduced stannic oxide single crystal. During the course of this present investigation on optical and semiconductive properties of reduced stannic oxide, an attempt was made to find the absorption due to free carriers in the infra red region beyond the edge of the intrinsic absorption.

Some work was also carried out to observe luminescence and electroluminescence in these crystals.

Section 2 Experimental Set Up and Measurement

(a) Grinding and Polishing

The crystals were first lapped into proper shape and geometry of a platelet. They were then mounted with "shellac" or durofix on steel disc of a Jig. (Fig. 5.1) The Jig has a circular rim at the bottom that keeps it levelled, where pressure can be applied through the sliding rod. The small steel disc at the bottom screws on to the central rod, and has a hole so that the

Fig 5.1 Crystals polishing Jig

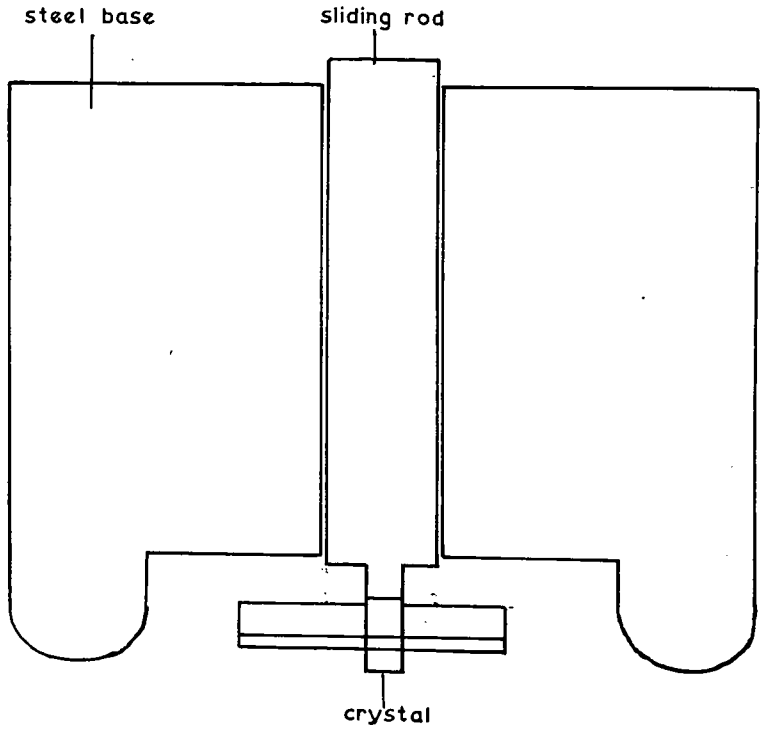

specimen can be examined in the polarizing microscope.

Grinding was done on plate glass using successively finer SiC or Alumina. The final polishing was done using diamond paste on a polishing pad mounted on a plate glass. Removal of the crystal from the disc was carried out by dissolving the cement by some suitable solvent.

(b) Spectrometers

Two different spectrometers were used for transmission measurement. SP-600 spectrophotometer was used in the beginning of the work, but it was abandoned later in favour of a better spectrometer.

Spectromaster:- This machine belongs to the Chemistry department, covers the range 0.6 - 25 μ but has a poor resolution. The principle of operation is such that the energy in the sample and the reference beam is kept equal by moving a 'comb' in and out of the reference beam. The scale can be adjusted by a second comb in the sample beam. When the instrument is used with the small area of a single crystal, a small hole in a blank is required in the reference beam.

Because of the similarity in dimension between the small hole and the teeth of the comb, the absorption scale is not likely to be linear.

The accuracy of the results depends to a large degree on the wavelength sensitivity of the spectromaster. This is stated in the instrument manual as follows:

	Accuracy	Repeatability
0.6 - 5 μ	0.002 μ	0.001 μ
5 - 15 μ	0.006 μ	0.002 μ

(c) Optical Absorption in Undoped Reduced Crystals

A number of measurements were made of free carrier absorption. In crystal 1, 5, 7 a continuous absorption was found between 1 and 5 μ which increased smoothly with wavelength. The carrier concentrations of these specimens were in the range $6.5 \times 10^{16} - 8 \times 10^{17}$ cm^{-3}.

Fig.(5.2), shows the variation of logarithmic absorption with logarithmic wavelength. It is evident from the graph that specimen 5 has a high absorption coefficient as it has more charge carriers than the others.

The slope for the specimen 5 is 2.6 while for the other crystals it is 2.5.

Fig. (5.3) shows the absorption coefficient variation with carrier concentrations at constant wavelengths.

FIG. 5·2 OPTICAL ABSORPTION

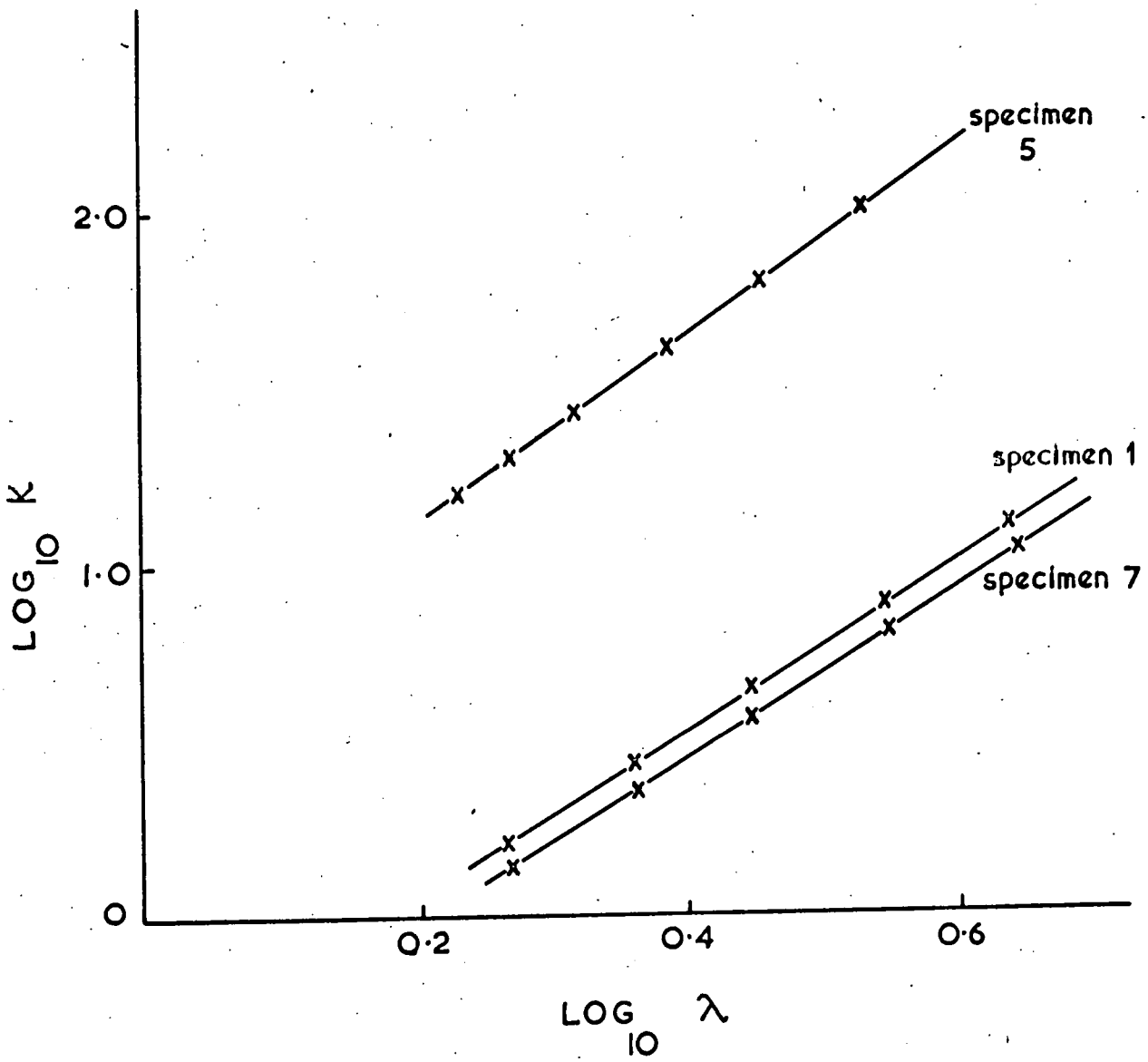

Fig 5.3 Absorption coefficient K (cm^{-1}) at constant wavelength V_s carrier concentrations

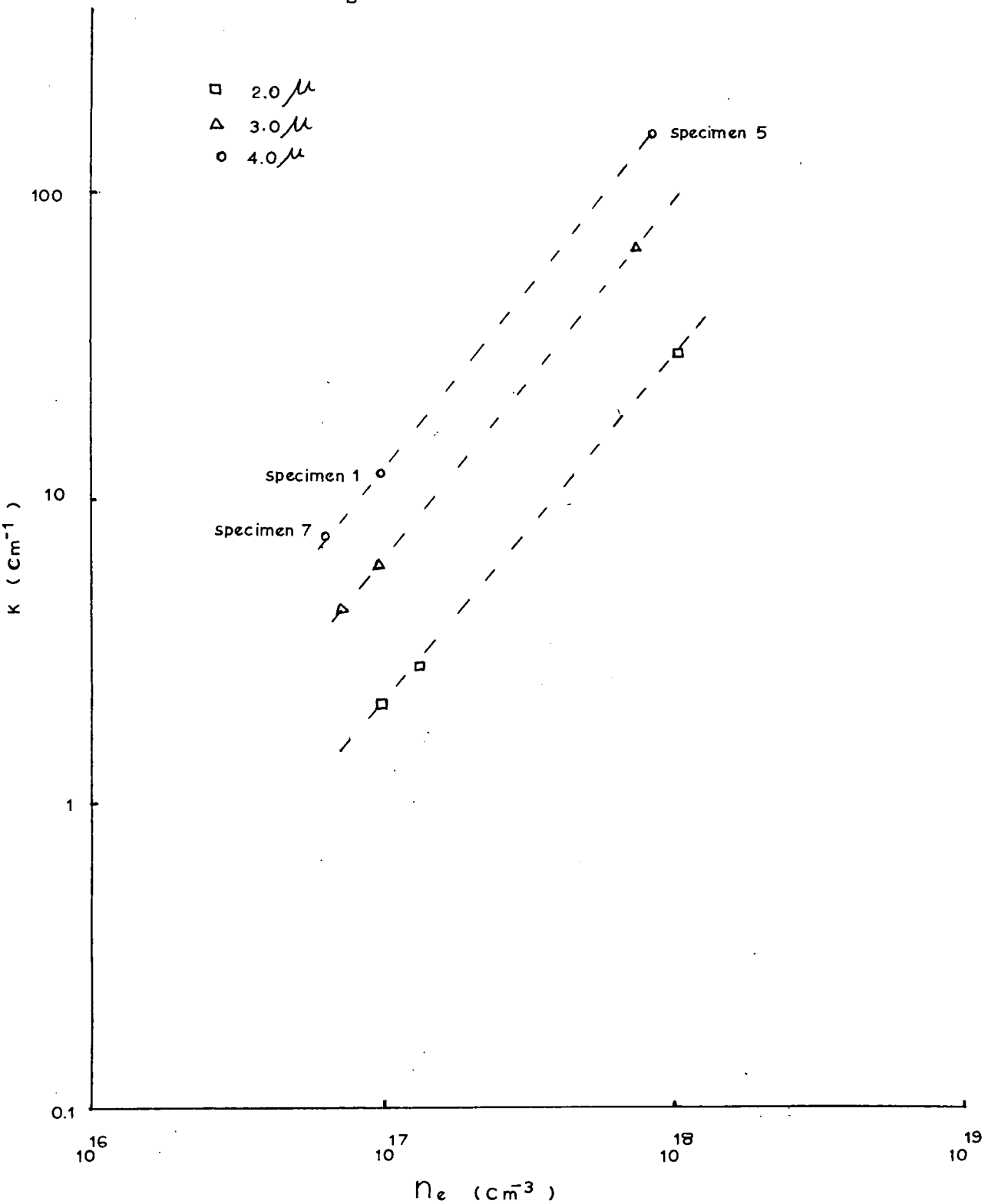

The general quality of these measurements was satisfactory due to specimen quality, specimen size and instrumentation. These crystals were found to be fairly pure and free from heavy microscopic voids or other defects that give a clear passage to the light.

As these grown crystals were subjected to reduction so there was homogeneity in conductivity in comparison to antimony doped crystals (see Chapter 6 Sect.3b). Discussion on the results of optical absorption is given in Chapter 6.

SUMMITT and BORRELLI (52) performed rather more extensive measurements in the wavelength range $0.5 < \lambda < 6\mu$ on antimony doped crystals with carrier concentration in the range 10^{17} - 2 x 10^{19} cm^{-3}. They found that for each specimen K varied as λ^{γ} where γ varied for different crystals from 2.9 to 3.3.

REDDAWAY (53) had also performed the same experiments in the wavelength range $0.8 < \lambda < 2.3\mu$ and carrier concentrations 3.6 x 10^{18} - 2 x 10^{19} cm^{-3}. He tested the relations $K \propto \lambda^{2}$ and $K \propto \lambda^{3}$, and found better agreement for the latter.

Section 3 (a) Luminescence

Crystals of stannic oxide grown by method A, B, or C (see Crystal Growth) and stannic oxide powder were examined under 2537 A^{o} Hg line irradiation. The antimony doped

crystals showed no luminescence, nor did the colourless undoped crystals.

These undoped transparent crystals and powder were reduced at 750°C at a pressure of 10^{-4} mm of Hg. When the above material was further excited by 2537 A° line a very bright luminescence with greenish white light was observed. This luminescence was seen at liquid nitrogen temperature, and it disappeared just below room temperature. No attempts to obtain the spectral distribution curve of the either undoped reduced crystals or the reduced stannic oxide powder were made.

(b) Electroluminescence

JEGES (54) first investigated the electroluminescent source of light in stannic oxide conducting crystal and powder. With an applied voltage of 5 to 300 volts D.C. and current ranging between millamperes and microamperes a white light was observed.

In the present work an attempt was made to observe the same effect. Experiments were done with different kinds of specimen namely doped, undoped, undoped reduced and powder stannic oxide, with wide range of conductivity between 10^{-5} to $3 \times 10^{\cdots}$ ohm^{-1} cm^{-1}.

The crystal was interposed between a pair of electrodes (Fig.5.3(a)). One of the electrodes was a metal (tungsten) needle, the point of which was in touch with the crystal body. The other electrode served as a holder of the crystal. The voltage was applied to the two electrodes and a white radiation was observed in the neighbourhood of the point of the needle. The voltage applied was varied from 10 to 70 volts while the current was ranging between 5 and 40 mA in different crystals.

The other experiment was performed on crushed powder of stannic oxide crystals. This powder was pressed between the two transparent conducting glasses as shown in Fig. (5.3b). A plastic frame served the purpose of fixing these conducting glasses. A direct current produced a white light in the powder which was confined to the corner, nearest the leads.

No white light or any kind of radiation was seen either in antimony doped, gallium doped or undoped crystals; light was observed only in reduced crystals.

One more experiment was done by preparing indium-gallium contact on one broad face of the stannic oxide crystal and the other face was subjected to cu-electroplating. With the passage of current no electroluminescence was obtained.

Fig. 5.3 (a)&(b) Demonstration of Electroluminescence

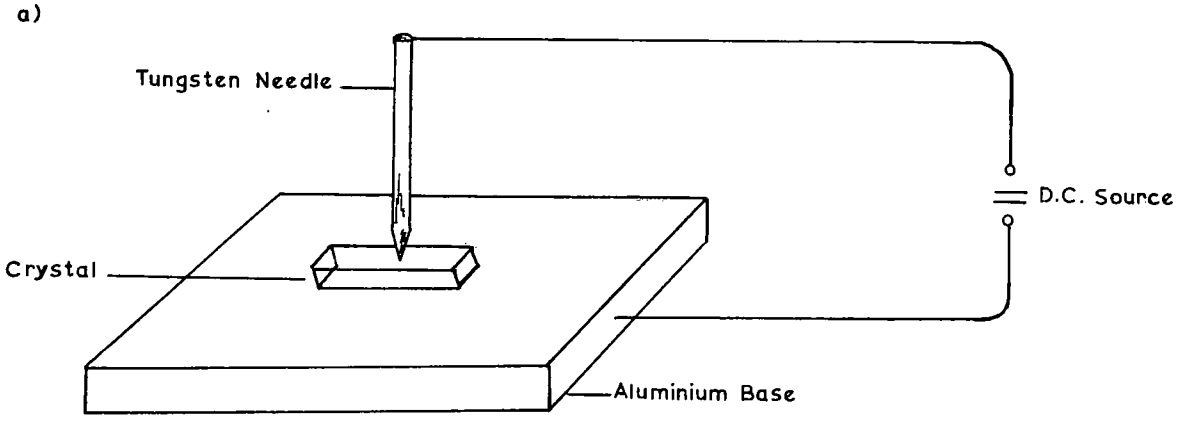

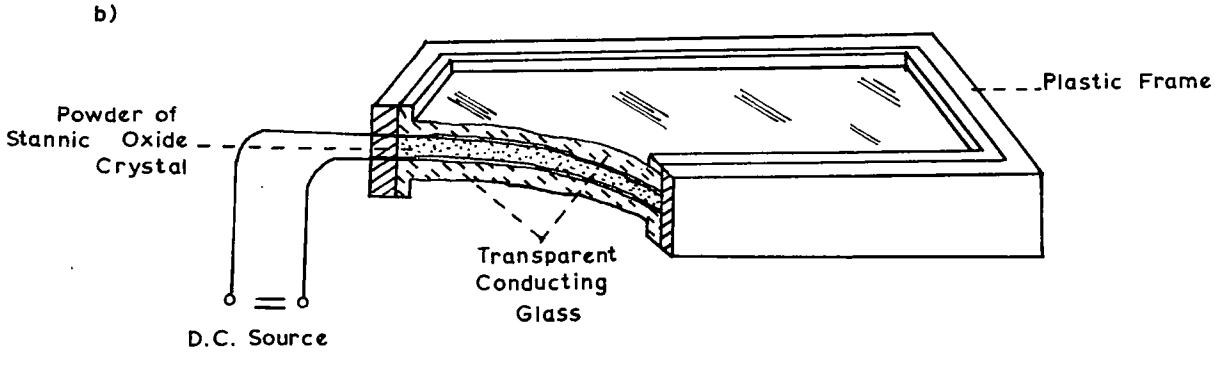

The reults of early experiments resembled those of JEGES (54), but when this effect was investigated at a pressure of 10^{-4} mm of Hg, the intensity of white light decreased to zero, so it was decided that all the light observed previously was due to a glow discharge in air at the contact, leading to some photoluminescence of the crystal. We believe that JEGES' results were due to the same effect.

CHAPTER 6

DISCUSSIONS AND CONCLUSIONS

Section 1 Introduction

Some investigations on the physical properties of SnO_2 have been carried out by different workers with thin films, sintered bodies and natural crystals (cassiterite). Data on the transport properties of SnO_2 have already led a number of authors to draw dissimilar conclusions concerning electron scattering mechanisms at low temperature.

Some of the present work gives further evidence on the scattering mechanism, as discussed below.

Section 2 (a) Mobility Measurements on Doped Crystals

Several antimony doped crystals were utilized for mobility measurements and the results on one crystal are shown in Fig.(4.4). From the results it is found that mobility decreases very slightly below 300°K down to 77°K. The same variation of mobility below room temperature was also observed in the crystals of MORGAN(5).

An explanation to these results was given by WRIGHT (45) that below 300°K the mobility is determined partly

by impurity scattering and below 100°K this must be entirely so. If the observed mobility is μ_o, the mobility determined by optical mode polar scattering μ_p, and the mobility determined by impurities μ_I then approximately

$$\frac{1}{\mu_o} = \frac{1}{\mu_p} + \frac{1}{\mu_I}$$

The writer has checked that the values of μ_I are of the order of those predicted using MANSFIELD's formula (20), assuming the above parameter, an impurity density of the order $10^{18}/cm^3$ and non degeneracy. It is clear from Fig.(4.4) that μ_p is very large compared with μ_o at low temperature so that $\mu_I \backsim \mu_o$.

(b) Mobility Measurements on Undoped Reduced Crystals below 300°K.

Fig.(4.3) gives the results of conductivity measurement with crystals in a temperature range from 77°K to 300°K. For crystals 1, 5 with increasing temperature from 77°K the conductivity increases very gradually, passing a maximum at 125°K and 200°K; it then decreases rapidly up to 300°K. For other crystals a continuous increase of conductivity was observed from 77°K to 300°K.

The measurements of Hall coefficient on crystal 1 showed that it increased rapidly as temperature fell below 125°K.

For undoped SnO_2, a positive temperature coefficient of the resistivity has not previously been observed below 300°K with sintered bodies or crystals except the crystals of NAGASAWA (14) and polycrystalline sample of VAN DALL (9).

In the present work, a positive coefficient is observed for crystals 1 and 5 in the range 125° - 300°K and 200° - 300°K respectively. Moreover, our latest measurements on crystal 13 (not mentioned in the present work) have shown that a continuous increase in conductivity is observed from 300°K to 77°K.

The values of conductivity Fig.(4.3) and Hall coefficient Fig.(4.6) lead to the temperature variation of mobility shown in Fig.(4.4).

For sample 1 this behaviour appears consistent with optical mode scattering, as discussed further below. The carrier density in this crystal is $10^{17}/cm^3$ at 300°K.

Taking the value of carrier concentration, and the value of electron effective mass 0.3 m (9), it

appears that the electron gas in the conduction band is probably non degenerate in the whole temperature region. 0.3 m_o is the value of effective mass, the writer believes to be correct, see Section 2(d) .

In crystal 2, the carrier concentration is about $10^{18}/cm^3$, so the mobility variation below 300°K is probably due to ionized impurity scattering with a further contribution due to optical phonons. Similar fall mobility below 300°K is seen in crystal 6 Fig.(4.4).

(c) Theoretical Interpretation of Mobility Results

MARLEY and DOCKERTY (43) showed, the theories of LEE LOW and PINES (34) and HOWARTH and SONDHEIMER (55) predict the values of mobility as shown in Fig.(6.1). The characteristic temperature was 500°K. The calculations leading to the values plotted have been checked and extended by the writer. A value of 1050°K (9) instead of 500°K gives the higher values of mobility as shown.

Fig.(6.1) shows the theoretical as well as experimental variation of mobility and there is reasonable agreement between the theory for θ = 500°K and the values obtained for crystal 1 between 77°K to 300°K. The small

Fig 6.1 Showing theoretical value of mobility

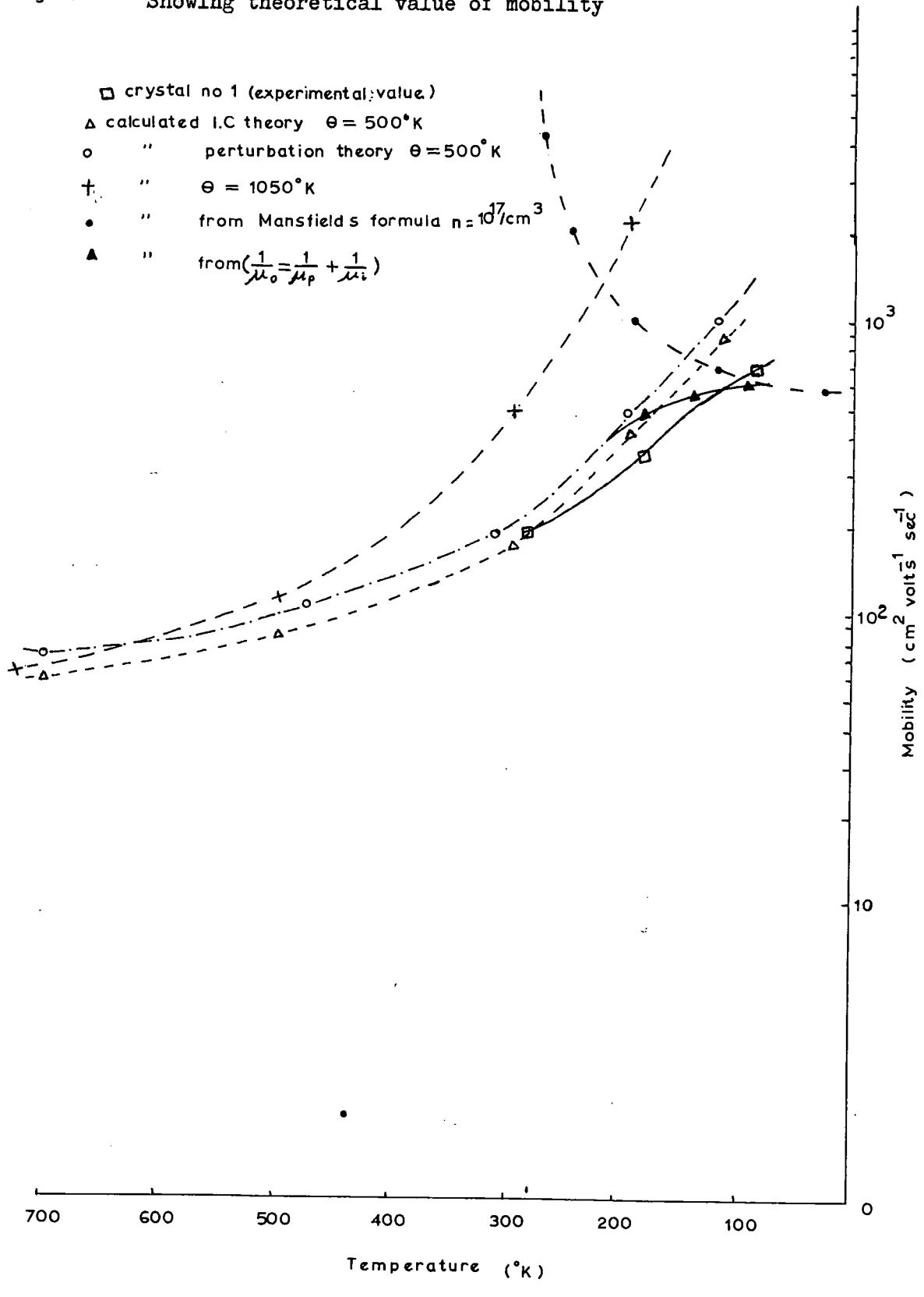

disagreement with crystal 1 may be due to slight contribution from impurity scattering; which is explained by the $\frac{1}{\mu_o} = \frac{1}{\mu_p} + \frac{1}{\mu_I}$ calculation, Fig.(6.1), assuming $m^* = 0.3\ m_o$; $\epsilon_\infty = 4$; $n = 10^{17}/cm^3$.

However for other crystals, Fig.(4.4), the optical phonon scattering is masked by ionized impurity scattering.

(d) Summary of Mobility Measurements

Fig.(III.1) (III.2) shows most of the published results of mobility measurements on stannic oxide. All these results show the same general trend. The mobility increases with increasing temperature up to about 300°K and then decreases with increasing temperature up to the highest value 600°K. The notable exception of this is result of reference (14), and (9).

The conclusions of KOCH (36), MARLEY and DOCKERTY (43), WRIGHT (45) and more recently by VAN DALL (9) indicate that the more important scattering mechanism at high temperature is polar optical mode vibrations.

If optical mode scattering is important in a polar crystal it is necessary to have an estimate of the coupling constant (α_c). REDDAWAY (53) has determined by optical

methods the wavelengths of optical modes of vibration. He proposes the most important value of wave number is 703 cm^{-1}; although if more than one mode is present in the crystal all modes will give some contribution toward the coupling constant.

If this value is used together with the value of electron effective mass 0.3 m_o (9); $\epsilon_\infty = 4$; $\epsilon_o = 15$ (9) a value obtained for α_c is 0.95. However if $\theta = 150^oK$ (36) so wave number is 120 cm^{-1}; then $\alpha_c = 3$. The true value probably lies near the first value of α_c .

VAN DAAL (9) confirmed the scattering mechanism and gave a value of α_c to be unity. He deduced that the electron effective mass lies between 0.2 to 0.3 m_o. The results of LYASHENKO and MILOSLAVSKII (32) indicated the effective mass (m*) is about 0.25 m_o at carrier density $\sim 10^{20}/cm^3$; they deduced lower value of m* at lower n.

If $\mu_H \propto T^{\varkappa}$, so MARLEY and DOCKERTY (43) obtained a value of $\varkappa$ of - 1.1 and greater than 3/2 for high temperature and low temperature respectively. They quote a value of effective mass (0.13 m_o) at 300^oK assuming ionized impurity scattering. An effective mass of 0.2 m_o is obtained if optical mode scattering is assumed.

The results of NAGASAWA (14) between 90°K and 300°K fits a curve μ_H = Constant $\times T^{-2}$ over the higher end of the temperature range. They quote a value of 0.3 m_o at 300°K based on acoustic mode scattering. An effective mass of 0.27 m_o is obtained if optical mode scattering is assumed.

(e) Discussion on Optical Absorption

The crystal defects generally believed important in free carrier absorption are acoustical phonons, optical phonons and ionized impurities.

We need not consider acoustical phonons since stannic oxide is a polar crystal, so our main concern will be with optical phonons. Ionized impurities are discussed further below.

The purity, and hence the high mobility of the crystal at room temperature indicate that absorption is due to polar optical modes. More over VISVANATHAN (60) gives $K \backsim \lambda^{2.5}$ for interaction with optical polar modes in 3 - 5 compounds, where optical phonon scattering seems to be more important scattering mechanism

The experimental value of r found from our optical absorption measurements lies very near to 2.5

(Chapter 5 Section 2c).

The expression given by VISVANATHAN for absorption due to optical mode scattering is as follows

$$\frac{K}{n_e}(cm^2) = \frac{4\pi}{nc}\,\frac{\sqrt{2}}{3}\,\frac{e^4\delta}{m^*}\,\frac{\hbar\omega_\ell^3}{(\hbar\omega)^3}\,(\hbar\omega)^{\frac{1}{2}}$$

$$\frac{(e^z+1)}{(e^z-1)} \times \left\{1 + \frac{11}{4\xi} - \frac{4}{(\pi\xi)^{\frac{1}{2}}} + \ldots\ldots\right\}$$

where $\delta = \epsilon_\infty^{-1} - \epsilon_o^{-1}$; $z = \frac{\hbar\omega_\ell}{KT}$

$\xi = \frac{\hbar\omega}{KT}$ and the other symbols have the usual meaning.

Calculations based on n = 2, $\omega_\ell = 1.6 \times 10^{14}$ cycle/sec (9) $\epsilon_\infty = 4$; $\epsilon_o = 15$ (9); $m^* = 0.3\ m_o$ (9) and $\lambda = 3\mu$ yields $\frac{K}{n_e}(cm^2) = 3.7 \times 10^{-17}$.

The experimental value of $\frac{K}{n_e}$ is 9×10^{-17} cm^2 at $\lambda = 3\mu$ for crystal 5. The mean for the three crystals is 7.10^{-17} cm^2.

It is important to mention here that with an effective mass of $0.13\ m_o$ (52) and $\epsilon_o = 25$; $\omega_\ell = 3 \times 10^{14}$

cycles/sec (52) the theoretical value of $\frac{K}{n_e}$ due to SUMMITT and BORRELLI is $9 \times 10^{-17} cm^2$. There appears to be no justification however for using such a high value of $\omega\tau$.

No optical absorption work is published on deliberately reduced crystals which state the absorption mechanism, while the present work agrees very well with VISVANATHAN (60), $\lambda^{2.5}$ variation.

The higher powers of λ, as obtained in the measurements of reference (52), (53) indicate some contribution of ionized impurities also. This is as expected theoretically from the work of VISVANATHAN (59) on 3 - 5 compounds. He also detected the increase in the power of λ with doping experimentally (60). The experiments of SUMMITT and BORRELLI at higher temperatures in (52) confirmed this explanation.

Section 3 (a) Nature of Defects and Reversible Heat Treatment

The heat treatment on as grown crystals (see Chapter 4 Section 3d) at low pressure raised the conductivity in these crystals. From the sign of the Hall voltage all the samples were found to show n type of conductivity. The donor centres responsible for n type conductivity are most probably oxygen vacancies.

An explanation of the n sign of

conductivity can be given as follows. The question of relative ionic size has been discussed by MANDEL (56), who has suggested that in certain compounds such as ZnO, ZnS, ZnSe, CdO, CdS, the increasing cation size promotes n type conductivity where as increasing anion size promotes p-type conductivity. The ratio of cation radius r_c to anion radius r_a describes the findings even better. In the case of SnO_2 the ratio $\frac{r_c}{r_a} \backsim 2.2$, so there is n type conductivity.

MANDEL's (56) theory which is based on a simple model can be applied here to explain our results. If an oxygen atom is removed from a SnO_2 crystal, resulting in a donor, a small vacancy cavity results. The wavelength of the standing wave is short, resulting in a high frequency and high energy of the state, and the carriers are high up in the potential box, corresponding to a low ionization energy.

It will be recalled that the ionization energy observed for donors in crystals 1 and 2 was 0.01 ev (see Table (4.2)).

The absence of conductivity in SnO_2 crystal after heating in an atmosphere of oxygen may be because any centres introduced have high activation energy. In addition to this, the theoretical calculations (5) based on fundamental

parameters give a value of 55 m_o for hole effective mass which also support our argument.

It is interesting to mention here that an experiment (Chap.4 Sec.3d) was performed to check the nature of centres. It was found that if a conducting crystal is heated in air at above about 1000°C, it becomes non conducting, while on reduction it became again conducting. A step by step reduction increased its conductivity but after a 45 hours treatment its mobility fell to half its value. This may be due to grain boundary effects.

Thus the results of oxidizing and reducing support the view that the donor centres are oxygen vacancies.

(b) Suggestion and Conclusion

There are at this stage a few papers on antimony doped single crystals but that work can not be of high value due to two factors. First it is too difficult to grow crystals of low impurity concentration $\sim 10^{17}/cm^3$, such that mobility will be governed by optical phonons at low temperature instead of impurity scattering. Moreover, the homogeneity of impurity in the crystal is very difficult to achieve.

A value of 20% variation in homogeneity is reported by MORGAN(5) by the thermoelectric probe method.

In the present work antimony doped crystals having electron densities with minimum values $6 \times 10^{17}/cm^3$ have been grown. These crystals were colourless rods or plates but having low mobility $\backsim 100$ cm^2 $volt^{-1}$ sec^{-1} at $300^{\circ}K$.

The undoped crystals which were fairly pure showed after reduction a mobility $\backsim 200$ cm^2 $volt^{-1}$ sec^{-1}. It is, however, very difficult to state at this stage the exact time and pressure to create a certain number of oxygen vacancies in the crystal which will control the mobility.

The most successful method of growth is so far due to NAGASAWA, in which there was a departure from stoichiometry in the as grown crystals. However the above work suggests the possibilty of changing the stoichiometric composition during or immediately after the growth process.

It is important to obtain a detailed knowledge of the band structure in order to investigate the electronic processes in SnO_2. Some work regarding the magnetoresistance in SnO_2 has been done by NAGASAWA (4), according to which the conduction band of SnO_2 consists of a single spheroidal energy valley situated at the origion of K-space.

This is consistent with his observation of direct exciton series at the edge of absorption spectrum of

SnO_2 (57). Summarizing the two results, he concluded that the top of the valence band and the bottom of the conduction band are located at the centre of the Brillion zone. His observation implies that the lowest energy transition is of direct type.

In the present work a magnetoresistance signal has been observed in one of our specimens at liquid air temperature. In future work the crystal 1 could be cut to give a [100] face and then NAGASAWA results could be checked. His results may be in error because he used a two probe method.

It is evident from our work that luminescence was observed in all our reduced crystals, but not in antimony doped or in undoped crystals which had not been reduced. The spectral energy curve for emission and absorption could be obtained at low temperature to find the defect centres responsible for the luminescence in these crystals.

No electroluminescence was observed from antimony doped or undoped crystals before reduction. Light output was obtained from reduced crystals, but we do not believe that it was genuine electroluminescence.

REFERENCES

1 I. Imai J.Phys. Soc. Japan 15, 937, (1960)

2 R.E. Aitcheson Australian J. Appl. Sci. 5, 10, 1954

3 W.A. Harrison Phy. Rev. 104, 1281, 1956

4 M. Nagasawa and Shigeo Shionoya Unpublished

5 D. Morgan Ph.D. Thesis 1966 University of Durham

6 H.F. Kunkle and E.B. Kohnke J. Appl. Physics 36, 1489, 1965

7 L.P. Kusmina and B.N. Litvin Soviet Physics Crystallography 8, 379, 1965

8 L. Clark and J. Woods Brit. J. Applied Physics 17, 319, 1966

9 H.J. Van Daâl Solid State Communication Vol.6 pp. 5 - 9 - 1968

10 G. Mandel Phys. Chem. Solids 23, 1177, 1962

11 H. Schafer Z. Anarg Chem. 286, 27 (1956)

12 H. Koch Physica Status Solidi 3, 1619, 1963

13 K. Ishigura, T. Sasaki, T. Arai, I. Imai J. Phy. Soc. Japan 13, 246, 1958

14 M. Nagasawa, S. Shionoya and S. Makishima Jap. Journal Applied Physics 4, 195, 1965

15 J.A. Marley and T.C. MacAvoy J. Appl. Physics 32, 2504, 1961

16 F.P. Koffyberg J. Appl. Physics 36, 844, 1965

17 T.B. Reed, J.T. Roddy and A.N. Mariano J. Appl. Physics 33, 1014, 1962

18 J. Bardeen and W. Schockley Phy. Rev. 80, 72, 1950

19 H. Brook Phy. Rev. 83, 879, 1951

20 R. Mansfield Proc. Phys. Soc. B69, 76, 1956

21 G.L. Pearson and J. Bardeen Phy. Rev. 75, 865 (1949)

22 C. Erginsoy Phy. Rev. 79, 1013 (1950)

23 D.L. Dexter and F. Seitz Phy. Rev. 86, 964, (1952)

24 G. Bauer Ann. d. Phys. 30, 433, 1937

25 R.H.W. Burkett J. British I.R.E. 21, 4, 301, 1961

26 L. Holland Vacuum Deposition of Thin Films p - 493f J. Wiley and Sons Ltd.

27 J.M. Mochel U.S. Patent 2, 522, 531

28 Handbook of Chemistry and Physics (edited by C.D. Hodgman), 46th. Edition P.E. 52 (1965-66)

29 T. Arai J. Phy. Soc. Japan 15, 5, (1960)

30 V.K. Miloslavskii Optics and Spectroscopy 7, 154, 1959

31 V.K. Miloslavskii and S.P. Lyashenko Optics and Spectroscopy 8, 455, 1959

32 S.P. Lyashenko and V.K. Miloslavskii Sov. Phys. Solid State 6, 2042, (1965)

33 S.P. Lyashenko and V.K. Miloslavskii Optics and Spectroscopy (U.S.A.) Vol.19, No.1 55 - 8 (July 1965)

34 F.E. Low and D. Pines Phy. Rev. 98, 414 (1955)

35 H. Koch Physica Status Solidi 3, 1059, 1963

36 H. Koch Physica Solidi 7, 263, 1965

37 I.F. Tigane Soviet Physics Solid State (U.S.A.) Vol.7, No.1, 212 - 3 (July 1965)

38 I. Golovcenco, G.I. Rusu, V. Stefan and M. Rusu An Strit Univ. "AI. I. CUZA" Iasi (Ser Nova) I (Rumania) Vol.11 No.1 77 - 80 (1965)

39 Golovcenco, Gh Ioan Rusin and V. Stefan An Strit Univ "AI. I. CUZA" Iasi (Ser Nova) I Rumania Vol.10, No.1 77 - 80 (1964)

40 Iachnimowski and Leja Acta Phy. Polon (Poland) Vol.30, No.1 (7) 45 - 9 July 1966

41 L.D. Loch J. Electrochem Soc. 110, 1081, 1963

42 E.E. Kohnke J. Phy. Chem. Solids 23, 1557, (1962)

43 J.C. Marley and R.C. Dockerty Phy. Rev. 140, A304, (1965)

44 M. Nagasawa, S. Shionoya and S. Makishima J.Phy Soc. Japan 20, 1093, 1965

45 D.A. Wright Proceedings of the British Ceramic Society No.10, March 1968

46 F. Van der Maesen and C.H.M. Whitmer Physics of Semiconductors Proc. 7th. International Conference Paris P1211, 1964

47 E. Conwell Physics Rev. 103, 47, 1956

48 G.T. Wright British Journal of Appl. Physics Vol.16, 1457, 1965

49 S.P. Mitoff J. Chem. Phy. 35, 852, 1961

50 A.C. Beer Galvonomagnetic Effects in Semiconductors p57, 1963

51 J.R. Drabble and R. Wolfe J. Electronics Control 3, 259, 1957

52 Summitt and Borrelli Journal of Phy. and Chemistry of Solids p.921, 26, 1965

53 S.F. Reddaway Ph.D. Thesis 1968, University of Durham

54 Karoly Jeges U.S. Patent Application Dec.17, 1954 Serial No. 475, 986

55 D.J. Howarth and E.H. Sondheimer Proc. Roy. Soc. A219, 3, 1953

56 G. Mandel I. Theory Phy. Rev. 134, A1073, 1964

57 M. Nagasawa and S. Shionoya Phys. Letters 22, 1966 409 - 410

58 H.J. Meyer Phys. Rev. 112, 298 (1958)

59 S. Visvanathan Phys. Rev. 120, 379 (1960)

60 S. Visvanathan Phy. Rev. 120, 376 (1960)